Phytochemistry 205 (2023) 113472

Contents lists available at ScienceDirect

Phytochemistry

journal homepage: www.elsevier.com/locate/phytochem

Glycine max (L.) Merr. (Soybean) metabolome responses to potassium availability

Gustavo dos Santos Cotrim, MSc. [a,d,*], Deivid Metzker da Silva, PhD. [b,d], José Perez da Graça, PhD. [c,d], Adilson de Oliveira Junior, PhD. [d], Cesar de Castro, PhD. [d], Guilherme Julião Zocolo, PhD. [e], Lucíola Santos Lannes, PhD. [a], Clara Beatriz Hoffmann-Campo, PhD. [d,**]

[a] São Paulo State University - UNESP, 15385-000, Ilha Solteira, SP, Brazil
[b] Santa Catarina Federal University - UFSC, 88040-900, Florianópolis, SC, Brazil
[c] Maringá State University - UEM, 87020-900, Maringá, PR, Brazil
[d] Brazilian Agricultural Research Corporation - Embrapa Soybean, 86001-970, Londrina, PR, Brazil
[e] Brazilian Agricultural Research Corporation - Embrapa Agroindústria Tropical, 60511-110, Fortaleza, CE, Brazil

ARTICLE INFO

Keywords:
Glycine max
Fabaceae
Potassium deficiency
Phytoalexins
Specialised metabolism
Abiotic stress
Metabolomics
Ionomics

ABSTRACT

Potassium (K^+) has vital physiological and metabolic functions in plants and its availability can impact tolerance to biotic and abiotic stress conditions. Limited studies have investigated the effect of K^+ fertilization on soybean metabolism. Using integrated omics, ionomics and metabolomics, we investigated the field-grown *Glycine max* (soybean) response, after four K^+ soil fertilization rates. Soybean leaf and pod tissue (valves and immature seeds) extracts were analysed by ultra-performance liquid chromatography coupled to high-resolution mass spectrometry (UPLC-HRMS) and inductively coupled plasma optical emission spectroscopy (ICP-OES). Multivariate analyses (PCA-X&Y e O2PLS-DA) showed that 51 compounds of 19 metabolic pathways were regulated in response to K^+ availability. Under very low potassium availability, soybean plants accumulated of Ca^{2+}, Mg^{2+}, Fe^{2+}, Cu^{2+}, and B in young and old leaves. Potassium fertilization upregulated carbohydrate, galactolipid, and flavonol glycoside biosynthesis in leaves and pod valves, while K^+ deficient pod tissues showed increasing amino acids, oligosaccharides, benzoic acid derivatives, and isoflavones contents. Severely K^+ deficient soils elicited isoflavones, coumestans, pterocarpans, and soyasaponins in trifoliate leaves, likely associated to oxidative and photodynamic stress status. Additionally, results demonstrate that L-asparagine content is higher in potassium deficient tissues, suggesting this compound as a biomarker of K^+ deficiency in soybean plants. These results demonstrate that potassium soil fertilization did not linearly contribute to changes in specialised constitutive metabolites of soybean. Altogether, this work provides a reference for improving the understanding of soybean metabolism as dependent on K^+ availability.

1. Introduction

Potassium (K^+) is an important macronutrient for plants' growing, and for playing a vital role in metabolic processes, as well for contributing to plants' adaptation to environmental stresses (Hasanuzzaman et al., 2018; Pandey and Mahiwal, 2020). However, it is well acknowledged that elevated concentrations of K^+ in the soil solution could competitively inhibit the uptake of Ca^{2+} and Mg^{2+} by plants (Mengel et al., 2001; Firmano et al., 2020; Keen and Taylor, 1975). Management programs to obtain high K^+ rates, or getting soils with high natural contents of K^+, can lead to a lower uptake of Mg^{2+} and, even Ca^{2+}, that generally triggers yield reductions (Castro et al., 2021) and, likely, inflicts remarkable metabolic consequences. Thus, the achievement of correct K^+ balance is very important factor for plants' development.

Many physiological and biochemical processes are dependent on K^+ availability, such as cell turgidity regulation, long-distance solute transport, enzymatic regulation (Amtmann et al., 2008; Huber and Arny, 1985), photosynthesis, protein synthesis, and membrane transport (Hafsi et al., 2014; Marschner, 2012). Balanced K^+ nutrition can promotes plant tolerance to stress conditions, as flooding (Mugnai et al.,

* Corresponding author.
** Corresponding author. Empresa Brasileira de Pesquisa Agropecuária – Embrapa Soja, Caixa postal: 231, 86001-970, Londrina, PR, Brazil.
E-mail addresses: gustavodscotrim@gmail.com (G.S. Cotrim), clarabeatriz.campo@embrapa.br (C.B. Hoffmann-Campo).

https://doi.org/10.1016/j.phytochem.2022.113472
Received 26 July 2022; Received in revised form 7 October 2022; Accepted 10 October 2022
Available online 19 October 2022

2011), low temperatures (Devi et al., 2012), drought (Wang et al., 2013), and salinity (Almeida et al., 2017). In contrast, K^+ deficiency in plants showed oxidative stress status (Hernandez et al., 2012; Hafsi et al., 2014; Hasanuzzaman et al., 2018), modifying heavily the biosynthesis of metabolites (Armengaud et al., 2009; Cui et al., 2019a, 2019b; Gaaliche et al., 2019).

Potassium is responsible for nearly 60 enzymes' activation taking part in carbon and nitrogen metabolism (Amtmann et al., 2008). In soils under adequate K^+ concentration, plants synthesise large biomolecules, as cellulose, starch, and proteins (Hasanuzzaman et al., 2018). Reversely, under K^+ deficiency the number of small molecules, as free sugars, amino acids, organic acids, and amides increases (Prasad et al., 2010). Also, it is necessary considers that the impact of K^+-supply in plants metabolism is multifaceted, tissue and species-specific, as observed in the responses to stresses in leaves and roots of tomatoes (Weinert et al., 2021), barley (Zhu et al., 2018), and oil palm sapling (Cui et al., 2019a, 2019b).

The prevalent view is that high K^+ availability decreases the severity of diseases or insect incidence in plants (Perrenoud, 1990; Severtson et al., 2016) and, thus, farmers are generally instructed to increase K^+ rates to improve crops' health (Potash Phosphate Institute, 1998; Gao et al., 2018; Seixas et al., 2020). In spite of the assumption that in most related cases K^+ fertilization decreases the incidence of the diseases, the opposite effect is also reported (Davis et al., 2018; Perrenoud 1990); experiments report 63% decrease and 28% increase in insect and mite incidence (Amtmann et al., 2008; Perrenoud, 1990).

Potassium deficiency has also significant effect on plant metabolism, including alterations in the profile, concentration, and distribution of many metabolites in different tissues (Amtmann and Rubio, 2012). Likewise, there is a consensus that specialised metabolites are crucial for plant susceptibility and defence against insects and pathogens (Amtmann et al., 2008; Davis et al., 2018; Gao et al., 2018). Nevertheless, how plants under K^+ contrasting availability can cope with biotic stresses remains unclear, and according to Marschner (2012), the understanding of the impacts of K^+ availability on specialised metabolism remains incipient when compared to the K^+ effect on physiological and on primary metabolism processes. An increase content of reducing sugars (primary metabolism) and of glucosinolates (specialised metabolite) potentially relevant to insects and/or pathogens was detected in *Arabidopsis thaliana* under K^+ deficiency, (Armengaud et al., 2009; Troufflard et al., 2010). Similarly, plants of *Hordeum vulgare* under K^+ deficiency increased jasmonic acid content and other oxylipins sensitive to the pathogen *Blumeria graminis* (Davis et al., 2018).

In *Glycine max* (L.) Merr. (Fabaceae), field experiments with K^+ fertilization revealed induction of multiple mechanisms improving plant resistance to cyst nematode *Heteroda glycines*, via root exudation of phenolic acids and plant pathogen-related genes (Gao et al., 2018). Furthermore, the metabolomic analysis revealed differences in gentisic acid and shikimic acid content from exudates of soybeans root, when plants are grown under low K^+ conditions (Tantriani et al., 2020). However, previous studies of soybean (*G. max*) metabolite content influenced by K^+ fertilization used only methodologies that allowed the detection of few target compounds (Hu et al., 2015; Seguin and Zheng, 2006; Vyn et al., 2002) or analytical methods covering primary metabolism (Tantriani et al., 2020). Certainly, these results improved our knowledge, but were not enough to understand how soybean under K^+ deficiency or adequate nutrition has constitutive specialised metabolites that can respond differently in plant interactions. Recently, studies comprising integrated omics greatly contributed for elucidating the influence of nutrients on soybean metabolism (Tantriani et al., 2020; Zhao et al., 2020). However, it remains unknown whether K^+ availability can impact the constitutive content of soybean specialised metabolites with a recognised role in biotic and abiotic interactions; thus, research methodologies based on untargeted metabolomics allow investigating of metabolome changes on a larger scale (Feng et al., 2020; Yang et al., 2018).

We hypothesize that K^+ rates in soil fertilization can promote an increase in specialised metabolite profiles of soybeans. This work aimed to advance a step towards understanding the effect of K^+ nutrition on soybean interactions, and we expected that these results could provide new insights into the importance of potassium in soybean metabolism. Therefore, we carried out untargeted metabolomics and ionomics analysis to compare the metabolic profile of trifoliate leaves and pod tissues (valves and immature seeds) of soybean influenced by K^+ availability. The contributions of this work allowed us to suggest the correlation of the soybean metabolite phenotype with K^+ status and list its importance previously reported in biotic and abiotic interactions.

2. Results and discussion

2.1. Soybean leaf ionomics analysis

Potassium leaf content increased in response to K^+ rates applied to the soil, as expected (Table 1). Potassium accumulation evaluated in very high K^+ soil availability (KVH) was 3.4-fold (16.22 g kg^{-1}) at upper third (UT), averaging 4.3-fold (12.08 g kg^{-1}) in medium third (MT) and lower third (LT) leaves, in comparison to very low K^+ availability (KVL) treatment (Table 1 and Table S2). Plant K^+ content was associated with soybean tissue maturity (Table 1 and Table S3). We observed that the upper third (UT) leaves had the highest K^+ levels compared to the MT and LT leaves, respectively. The high mobility of potassium was previously reported by Marschner (2012) and Mengel et al. (2001) who also related that due to higher demand for K^+ in metabolic activities, potassium is often transported, redistributed, and accumulated primarily for the young tissues.

Leaf calcium (Ca^{2+}) and magnesium (Mg^{2+}) contents decreased significantly with increasing K^+ rates; phosphorus (P) and sulphur (S) levels were not altered by treatments (Table 1). However, the mean content of S tended to be higher in MT and UT (> 2.0 g kg^{-1}), compared with the LT (Table 1 and Table S3). Other authors reported a reduction in Ca^{2+} and Mg^{2+} content by increases in K^+ soil fertilization (Diem and Godbold, 1993; Firmano et al., 2020; Hafsi et al., 2014); this effect has been associated with luxury K^+ consumption and competitive inhibition of the root absorption sites. According to Hafsi et al. (2014) the uptake of Mg^{2+} and Ca^{2+} detected in leaves under K^+ deficiency can be associated with alleviating the effects of nutritional deficiency.

The contents of micronutrients, as manganese (Mn^{2+}), iron (Fe^{2+}), copper (Cu^{2+}), and boron (B) in old leaves (LT) of soybean plants significantly increased by 1.04-, 1.11-, 1.23-, and 1.88-fold under KVL compared to KVH (Table 1). Regardless of treatments, Fe^{2+} and Mn^{2+} concentrations were lower in MT and UT leaves in comparison to LT (Table 1 and Table S3). However, zinc (Zn^{2+}) leaf content in the three growing regions (LT, MT, and UT) was reduced when soybean plants grown under very low potassium availability (KVL).

These experimental results suggest that soybean leaves might resist low potassium availability by accumulating Ca^{2+}, Mg^{2+}, Mn^{2+}, Fe^{2+}, Cu^{2+}, and B. Integrated omics of wild soybean (*Glycine soja*) under low phosphate availability showed an accumulation of Ca^{2+}, Mg^{2+}, Fe^{3+}, NO_3^- and S in young leaves, and reduced Zn^{2+} levels as related by Shen et al. (2021). The results of Shen and collaborators concerning to soybean under low P availability had the same tendency as our nutrient availability data investigating K^+ deficiency, suggesting this interaction (P and K^+ deficiency) should be investigated in the future to understanding the mechanisms of soybean tolerance to deficiency of nutrients.

Iron usually acts as a mineral regulatory element and defends plants against stresses by activating plant enzymatic antioxidants (Tripathi et al., 2018). The reduction in boron contents in soybean leaves in condition of increased K^+ rates (Table 1) was probably associated to its low phloem mobility (Marschner, 2012). Moreover, reductions of B availability may also occur due to low Ca^{2+} uptake, revealed in plants that grown under high K^+ soil content, which reduced the B requirement (Firmano, 2017; Firmano et al., 2020). In general, our results

Table 1
Ionomic analysis of soybean trifoliate leaves (cv. BRS 1010 IPRO) in response to K^+ soil fertilization.

Treatments		Leaf DW	P	K^+	Ca^{2+}	Mg^{2+}	S	Zn^{2+}	Mn^{2+}	Fe^{2+}	Cu^{2+}	B
		(g)	($g\ kg^{-1}$)					($mg\ kg^{-1}$)				
KVL	LT	0.22	2.47aB	2.73cB	22.9aA	11.37aA	1.67aB	43.17bA	279.72aA	398.17aA	12.30aA	64.75aA
KL	LT	0.24	2.44aB	7.25bB	19.9aA	5.78bA	1.75aB	50.83aA	282.28aA	389.08bA	9.95bA	38.59bB
KM	LT	0.25	2.39aB	8.84bB	14.5bA	4.17cA	1.65aC	51.39aA	270.50bA	353.50cA	8.95bA	37.67bB
KVH	LT	0.25	2.41aB	12.02aB	12.0bA	3.27cA	1.62aB	50.39aA	268.44bA	358.17cA	9.95bA	34.32bB
KVL	MT	0.31	2.60aA	2.87cB	20.1aB	9.38aB	2.27aA	35.94bB	248.22aB	269.33aB	10.60aA	58.38aA
KL	MT	0.37	2.62aA	7.97bB	16.2bB	5.07bB	2.23aA	44.44aB	251.61aB	226.50bB	9.60aA	37.33bB
KM	MT	0.35	2.59aA	9.40bB	12.2cA	3.67cB	2.14aB	46.50aB	246.61aB	200.67cB	8.22aA	29.90cC
KVH	MT	0.36	2.56aA	12.14aB	11.5cA	3.02cB	2.16aA	47.06aB	254.06aB	196.17cB	8.57aB	30.85cB
KVL	UT	0.38	2.60aA	4.70dA	17.2aC	7.75aC	2.39aA	25.06bC	137.28aC	263.16aB	11.07aA	61.95aA
KL	UT	0.44	2.61aA	9.88cA	11.0bC	3.53bC	2.37aA	28.00aC	133.44aC	221.83bB	9.32bA	44.48bA
KM	UT	0.44	2.57aA	13.64bA	9.60cB	3.07bC	2.31aA	28.56aC	128.50aC	182.67cB	8.18bA	41.35bA
KVH	UT	0.43	2.53aA	16.22aA	9.50cB	2.78bB	2.37aA	27.89aC	130.06aC	183.19cB	7.48bC	39.75bA

Leaf DW – leaf dry weight; KVL – very low K^+ availability; KL – low K^+ availability; KM – medium K^+ availability; KVH – very high K^+ availability; LT – lower third; MT – medium third; UT– upper third; The data presented are representations of the mean ($n = 6$) and results of ANOVA + Tukey's test ($p \leq 0.05$); Different lower case letters indicate differences amongst K^+ availability conditions (KVL, KL, KM, and KVH) in the same soybean tissue; Different capital letters indicate differences amongst soybean trifoliate leaves (LT, MT, and UT) in the same K^+ treatment.

demonstrate that the content of Mn^{2+}, Zn^{2+}, and Cu^{2+} in the leaves are poorly or non-responsive to increasing K^+ levels in the soil. In fact, the concentration of these nutrients in soybean leaves (cv. BRS 1010 IPRO) was also not affected in the agronomic assays reported by Firmano (2017), being within or above the class of contents considered appropriate (Harger, 2008).

2.2. Soybean pod ionomics analysis

Ionomics analysis showed that the K^+ content increased 1.65-fold (11.7 g kg^{-1}) in immature seeds (IS), and 5.0-fold (12.5 g kg^{-1}) in pod valves (PV) when KVH treatment was compared to KVL (Table 2 and Table S4). The increased of K^+ content in immature seeds in KVH and KVM was similar but higher than that assimilated by IS of plants under KL and KVH treatments. In general, our results obtained for K^+ accumulation in soybean seeds were similar to those reported by Parvej et al. (2015) and Vyn et al. (2002). The seeds, as propagation organs of the species, tend to receive a greater nutrient amount, even in plants in a nutritional deficiency status (Marschner, 2012).

The pod valves are more affected by low potassium availability (KVL and KL treatments); they presented mean levels of K^+ accumulation > 2.50 g kg^{-1}, compared with immature seeds (> 7.07 g kg^{-1}). Other macronutrients (P, Ca^{2+}, Mg^{2+}, and S) were not significantly altered by treatments in soybean pod tissues. In general, the P content observed in IS (< 3.23 g kg^{-1}) is higher than detected in PV (< 2.63 g kg^{-1}) by two-sample *t*-test, except in the KM-PV *vs.* KM-IS (Table 2 and Table S5). However, the accumulation of Ca^{2+} and Mg^{2+} was greater in PV (> 7.03 and 3.73 g kg^{-1}, respectively).

The concentration of Zn^{2+} and Mn^{2+} were higher in the PV (> 65.6 mg kg^{-1}) of soybean plants in soils with medium (KM) and very high potassium (KVH) availability (Table 2). The same tendency was only observed for Mn^{2+} in IS. These results indicated that low K^+ soil availability increased Mn^{2+} accumulation in soybean pod tissues (R5.5 stage). Copper content (Cu^{2+}) responded only in pod valves when soybean plants were exposed to very low and low potassium treatments (KVL and KL). Immature seeds (IS) showed increased Fe^{2+} concentration in KVL compared to other K^+ treatments (< 53.6 mg kg^{-1}). Under our experimental conditions, no significant changes in the content of Zn^{2+}, Cu^{2+} and B were observed in IS, and Fe^{2+}, and B in PV considering the four potassium availability conditions (Table 2).

The effect of potassium availability on the elemental content of vegetative and reproductive tissues from our results showed that Ca^{2+} and Mg^{2+} responded to K^+ rates only in leaves; this interaction did not occur in soybean pod tissues (R5.5 stage). Furthermore, plants grown under very low and low potassium content (KVL and KL) did not accumulate Ca^{2+}, Mg^{2+}, Mn^{2+}, and B in pod tissues, as observed in the results of trifoliate leaves (especially LT leaves). However, Cu^{2+} increased concentration occurred only in pod valves and leaves under low K^+ availability (Table 1 and Table 2), and Fe^{2+} content only responded to immature seeds in comparison to pod valves.

An increase in K^+ fertilization, as reported by Firmano et al. (2020) provided greater Mn^{2+} accumulation in soybean seeds, with

Table 2
Ionomic analysis of soybean pods (cv. BRS 1010 IPRO) sampled at R5.5 growth stage in response to K^+ soil fertilization.

Treatments		P	K^+	Ca^{2+}	Mg^{2+}	S	Zn^{2+}	Mn^{2+}	Fe^{2+}	Cu^{2+}	B
		($g\ kg^{-1}$)					($mg\ kg^{-1}$)				
KVL	PV	2.63aB	2.50dB	7.03aA	4.47aA	1.06aB	6.83cB	33.00cA	69.33aA	10.27aB	27.13aA
KL	PV	2.55aB	5.13cB	7.37aA	4.47aA	1.13aB	9.97bA	40.67bA	71.67aA	10.57aB	29.30aA
KM	PV	2.57aA	10.53bA	9.50aA	3.93aA	1.19aB	11.20aA	68.67aA	68.67aA	8.70bB	34.30aA
KVH	PV	2.53aB	12.57aA	8.37aA	3.73aA	1.05aB	13.60aA	65.67aA	71.33aA	7.53bB	31.77aA
KVL	IS	3.23aA	7.07bA	2.37aB	1.53aB	1.76aA	11.43aA	24.00bB	58.67aA	21.73aA	15.97aB
KL	IS	3.14aA	7.87bA	2.37aB	1.43aB	1.73aA	10.50aA	23.67bB	51.67bB	18.97aA	15.73aB
KM	IS	3.15aA	11.47aA	2.47aB	1.50aB	1.91aA	12.83aA	36.00aB	52.33bB	20.23aA	17.52aB
KVH	IS	3.12aA	11.73aB	2.43aB	1.50aB	1.87aA	11.70aA	35.00aB	53.67bA	19.50aA	17.87aB

KVL – very low K^+ availability; KL – low K^+ availability; KM – medium K^+ availability; KVH – very high K^+ availability; IS - immature seeds; PV – pod valves; The data presented are the mean values ($n = 6$); Different lower case letters indicate differences amongst K^+ availability conditions (KVL, KL, KM, and KVH) in the same soybean tissue by Tukey's test ($p \leq 0.05$); Different capital letters indicate differences amongst soybean pod tissues (PV and IS) in the same K^+ treatment by two-sample *t*-test ($p \leq 0.05$).

stabilization of this concentration after soil rate fertilization (> 120 kg K_2O ha^{-1}). The Mn^{2+} increase content in IS can be associated with its activity in energetic metabolism (Malvi, 2011). The high K^+ availability can promote the major metabolic activity in plants, which leads to greater Mn^{2+} content in seeds (Firmano, 2017). Overall, our results are consistent in the relationship of nutritional balance of macro and micronutrients when soybean plants were under the contrasting conditions of K^+ availability (Marschner, 2012).

2.3. Yield parameters

The dry weight of 100 seeds and the yield parameters increased with the K^+ rates (Table 3). Both variables were positively related to K^+ availability, and 100-seed dry weight was higher, as expected, in the KVH (15.5 g) and KM (15.4 g) than in the KL (14.0 g) and KVL (12.3 g) treatments. The yield followed the same trend; the highest means was achieved by KVH (4095.6 kg ha^{-1}), and KM (4092.6 kg ha^{-1}) treatment plots, in contrast to KL (3736.9 kg ha^{-1}) and KVL (2211.0 kg ha^{-1}). Parvej et al. (2015) related yield increase of 40 and 60% when soybean grown under medium and high K^+ soil fertility (81 and 91 mg K^+ kg^{-1}, respectively), compared with the low K^+ treatment (61 mg K^+ kg^{-1}). A previous study in the same edaphoclimatic conditions of ours conducted by Firmano et al. (2020) showed that soybean yield stabilised when the K^+ soil content extracted by Mehlich-1 reaches 0.15 $cmol_c$ dm^{-3}. In our analysis, the potassium soil concentration in KM treatment was 0.13 $cmol_c$ dm^{-3}, and 0.50 $cmol_c$ dm^{-3} in KVH (Table S1), justifying the similarity between soybean yields observed in both treatments.

2.4. Chemometrics analysis

In our study, we established two-blocks (X = intensities of metabolites; Y = ion concentration). PCA-X&Y_A was created for trifoliate leaf samples and shows 404 variables (Fig. 1a). The Pareto scale scored 21 components, explained by 83% $R^2X_{(cum)}$ variance. The first two main components accounted for 45.3% of the total variance (R^2X [1] = 0.317 and R^2X [2] = 0.136). PCA-X&Y_A also showed distant points representative of the leaf growth regions (LT, MT, and UT) in PC1. The O2PLS-DA_B model exhibited similar clustering, with better separation of the treatments in leaf samples (Fig. 1b). Cluster I has 9.1 to −14.5 variance in PC2, and in general, the O2PLS-DA_B score plot showed two main components, cluster I (KL, KM, and KVH) and cluster II (KVL), observable by PC2.

Loading plots of trifoliate leaves reveal the influence of K^+ content measured by ionomic analysis (Fig. 1c), as previously reported (2.1 section). Potassium fertilization had a greater contribution to cluster I (KL, KM, and KVH), predominantly on the upper third (UT) leaves in both treatments (Fig. 1b and Fig. 1c); Zn^{2+} and Mn^{2+} content also contribute to PC2, but mostly for the lower third (LT) and medium third (MT) leaves. The concentration of Ca^{2+}, Mg^{2+}, Cu^{2+}, Fe^{2+}, and B were associated with the leaves of plants that grow under very low potassium availability (KVL).

Table 3
Soybean (cv. BRS 1010 IPRO) grains yield parameters as function of K^+ soil availability.

Treatments	100-Seeds DW (g)	Yield (kg ha^{-1})
KVL	12.37c	2211.0c
KL	14.06b	3736.9b
KM	15.56a	4092.6a
KVH	15.47a	4095.6a

KVL – very low K^+ availability; KL – low K^+ availability; KM – medium K^+ availability; KVH – very high K^+ availability. The data presented are the mean values ($n = 6$) obtained from ANOVA. Means followed by the same letter in the column do not differ by Tukey's test ($p \leq 0.05$).

In the PCA-X&Y D model, the pod tissue samples dataset used was composed of 221 variables, with seven components explaining 89% of the variance in $R^2X_{(cum)}$ (Fig. 1d). Two main components explained 75.4% of the variance (R^2X [1] = 0.697 and R^2X [2] = 0.057), revealing low treatment separation characteristics for PC2. Pod valves (PV) and immature seeds (IS) samples were distant from the projection (PC1). The use of O2PLS-DA_E (supervised model) was necessary to treatments distinctions (Fig. 1e) since only PCA-X&Y_D did not clearly explain the relationship between the K^+ rates and metabolite content in pod tissues. The clusters in the supervised multivariate model (O2PLS-DA_E) from the pod tissues and the results of ANOVA (Tukey's test) were similar in regard to K^+ availability (Table 2). Four groups were observed in O2PLS-DA_E score plot, cluster I (KM-IS and KVH-IS), cluster II (KL-IS and KVL-IS), cluster III (KM-PV and KVH-PV), and cluster IV (KL-PV and KVL-PV), represented by Fig. 1e.

Chemometric models showed that K^+ rates applied in soil fertilization were represented by PC2, while different sampling leaf regions (LT, MT, and UT) and pod tissues (PV and IS) were explained by PC1 (Fig. 1). The positive quadrant of PC2 in the plot of IS and PV metabolic profiles reveals that medium and very high potassium availability (KM and KVH) treatments showed a correlation of K^+ content measured in ionomic analysis (Fig. 1f). However, the variance between the K^+ availability (KVL, KL, KM, and KVH) was significantly lower in pod tissues (3.33% by PC2; Fig. 1e) compared to trifoliate leaves (11.5% by PC2; Fig. 1b). These results suggest that potassium rates promote more variance in leaf metabolite content than in pod valves and immature seeds, respectively.

The O2PLS-DA model (Table S6), established from the metabolomics/ionomics datasets for soybean leaves and pods, explained 99% $R^2Y_{(cum)}$ e predicted 98% $Q^2Y_{(cum)}$ of the total variance, indicating the adequacy of the model, and allowing the establishment of S-Plot graphs, using only KVL *vs.* KVH treatments. We observed that soybean under very high potassium availability (KVH) accumulated differentially 17 and 7 compounds in leaves and pods, respectively, compared with the lowest K^+ availability (Table 4 and Table 5). Under very low potassium availability, O2PLS-DA models (KVL *vs.* KVH) revealed that 21 and 18 metabolites were upregulated in trifoliate leaves and pod tissues, respectively (Table 6 and Table 7). These experimental results indicated that K^+ rates did not contribute to linearly increasing in the content of constitutive specialised metabolites in soybean development stages sampled, rejecting our initial hypothesis. However, our data showed that under very low potassium availability soybean metabolism had the highest metabolic shift, as also observed previously by Shen et al. (2021) with *G. soja* deficient in phosphorus.

The multivariate analysis grouped the leaf samples according to the growth region (LT, MT, and UT). The progressive metabolite accumulation may be a response to observed differences in tissue maturity, also reported by Song et al. (2014) and Yuk et al. (2011). These authors associated the expressive accumulation of coumestrol and glyceollin VII in soybean leaves at R7/R8 stages. Likewise, wild soybean under low inorganic phosphate (Pi) conditions promoted the transportation and reuse of sugars and amino acid metabolites and mobilize Pi from hexose-phosphate from old to young leaves (Shen et al., 2021). Unlike K^+, phosphorus is a structural component of many molecules in plants, which justifies major metabolome reprogramming. However, potassium in plants is more associated with catalysis or activation of enzymes (Cui and Tcherkez, 2021; Marschner, 2012). Soybean under potassium homeostasis should have a sufficient level of this nutrient for enzymatic activity, not resulting in an increase in the contents of constitutive specialised metabolite, as shown by our experiment. Otherwise, K^+ deficiency leads to relevant metabolic changes (Lu et al., 2019; Troufflard et al., 2010), as also observed to low nitrogen (Liu et al., 2019) or phosphorus (Shen et al., 2021) conditions.

2.5. Molecular networking and metabolic pathway

Feature-based molecular networking analysis (FBMN) was carried

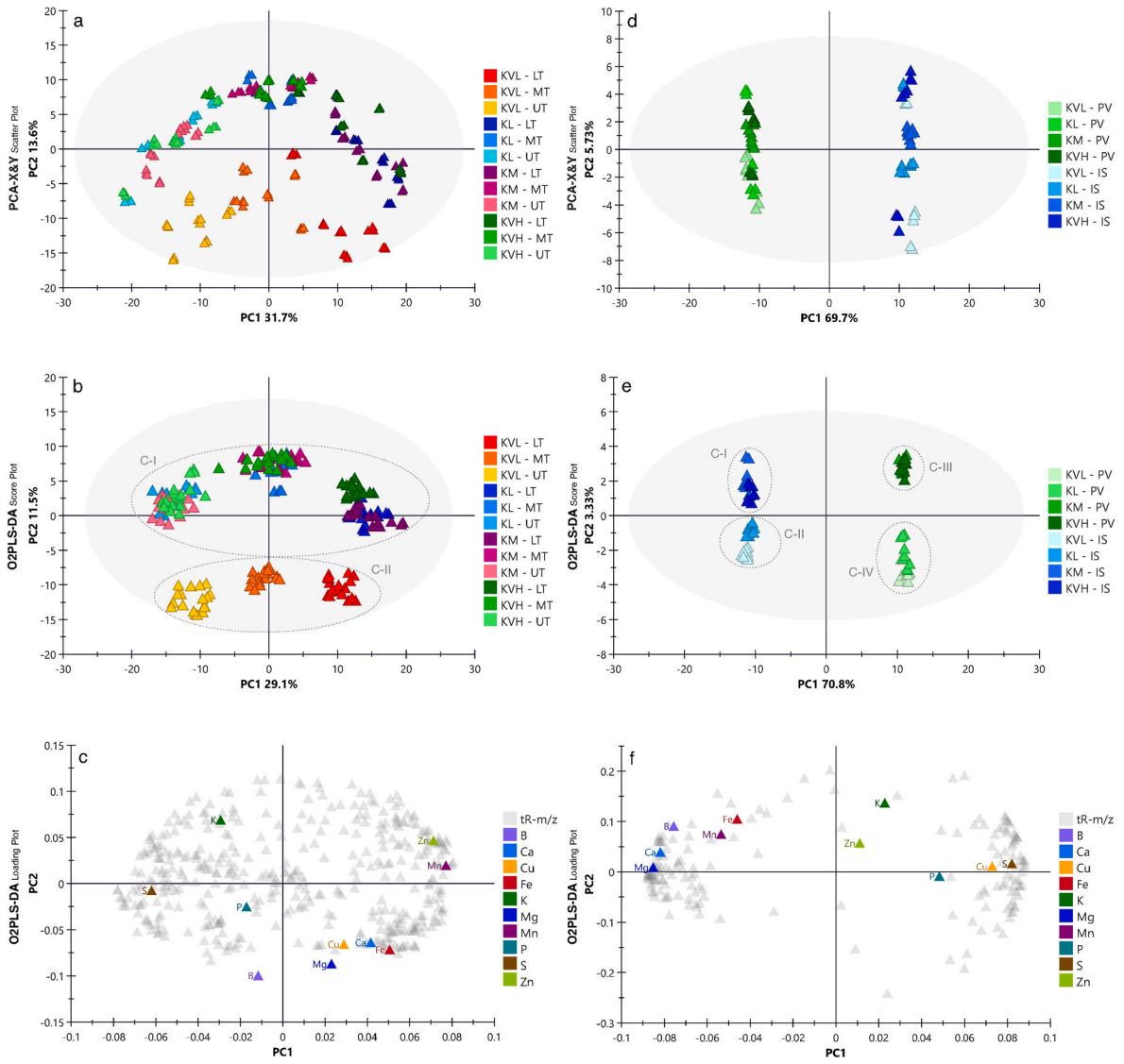

Fig. 1. Unsupervised and supervised chemometric models of UPLC-QTof-MS^E data of soybeans under four soil K^+ availability. These models allowed us to correlate the metabolomics data (404 and 221 molecular features to soybean leaves and pod tissues, respectively as X input) with ionomics (10 factors as Y input) coherently. (a) PCA-X&Y_A scatter plot of trifoliate leaves. (b) O2PLS-DA_B score plot highlighting the identified two clusters (C–I and C-II) of trifoliate leaves. (c) O2PLS-DA_B loading plot of trifoliate leaves, the loadings (factor) in the graph represents macro and micronutrients quantified by ICP-OES that contribute to the O2PLS-DA model. (d) PCA-X&Y_D scatter plot of soybean pod tissues. (e) O2PLS-DA_E score plot highlighting the identified four clusters (C–I, C-II, C-III, and C-IV) of soybean pod tissues. (f) O2PLS-DA_E loading plot of soybean pod tissues, the loadings (factor) in the graph represents nutrients quantified by ICP-OES that contribute to the O2PLS-DA model. List of abbreviations: LT – lower third leaves; MT – medium third leaves; UT– upper third leaves; IS - immature seeds; PV – pod valves; KVL – very low K^+ availability; KL – low K^+ availability; KM – medium K^+ availability; KVH – very high K^+ availability.

out to gain comprehensive overview of the differentially regulated metabolites in response to K^+ availability, complementing that data indicated by base peak intensity (BPI) in chromatograms and the differential chemical profile of soybean tissues (Fig. 2). The dataset containing MS/MS spectra of 902 features obtained from the soybean trifoliate leaf and pod tissue samples was organised into a single molecular network. In this approach, the nodes representing each spectrum were organised into 89 clusters of different families of molecular structures (Fig. 3). The FBMN, in our study, was performed with data export from MS-DIAL software, which considers adducts and possesses a spectrum dereplication method which is not exactly the same as MarkerLynx software. Consequently, as MarkeLynx does not consider adducts, different numbers of molecular features (t_R-*m/z*) were observed. Therefore, the compounds were annotated in the molecular network through automated library spectral by matching approaches. The difference observed between 625 molecular features (t_R-*m/z*) from the multivariate analysis and 902 nodes represents other different forms of ionization possible in our chromatographic conditions (adducts).

The features highlighted by chemometric analysis were identified and colour-coded in the molecular network. This strategy allowed us to highlight the compounds impacted by K^+ availability and relate them to chemical structures. Spectra not clustered into molecular families were represented as self-loop nodes at the bottom of the network; coloured nodes represent ontology groups of soybean metabolites regulated by K^+ fertilization. Lack of comprehensive spectral libraries associated with characteristics of our MS^1 and MS^2 data (MS^E/DIA – data-independent acquisition) can explain the considerable number of spectra not clustered.

The chemical ontology analysis of metabolites influenced by K^+ fertilization showed regulation of sixteen phenolic compounds, members of the groups of flavonols, isoflavones, coumestans, and pterocarpans; eight lipids classified as jasmonic acid conjugates, fatty acids,

Table 4
Putative metabolite identification from soybean leaves upregulated under very high potassium (KVH) availability by UPLC-QTof-MS^E.

t_R (min)	Formula	Identification	Chemical Ontology	Lower Third (LT)			Medium Third (MT)			Upper Third (UT)		
				KVL-LT *vs.* KVH-LT			KVL-MT *vs.* KVH-MT			KVL-UT *vs.* KVH-UT		
				FC	FDR	VIP	FC	FDR	VIP	FC	FDR	VIP
0.66	$C_{12}H_{22}O_{11}$	Sucrose	Carbohydrates	––	––	––	2.1	$4.17E^{-02}$	2.2	3.3	$4.00E^{-02}$	1.8
0.73	$C_5H_{10}O_5$	D-xylose	Carbohydrates	16.1	$3.57E^{-03}$	1.6	15.1	$4.17E^{-03}$	1.7	11.7	$3.33E^{-03}$	1.2
0.73	$C_4H_6O_5$	Malic acid	Beta hydroxy acids	7.8	$7.14E^{-03}$	1.2	9.9	$1.25E^{-02}$	1.3	2.1	$3.33E^{-02}$	0.7
3.40	$C_{33}H_{40}O_{21}$	Kaempferol-3-glucosyl-(1 → 2)-gentiobioside	Flavonols	1.4	$1.79E^{-02}$	2.2	1.4	$3.33E^{-02}$	2.2	1.4	$5.00E^{-02}$	1.1
4.35	$C_{27}H_{30}O_{15}$	Kaempferol-3-*O*-*α*-L rhamnopyranosyl-(1 → 6)-*β*-D-galactopyranoside	Flavonols	4.9	$1.07E^{-02}$	1.7	4.8	$8.33E^{-03}$	2.1	5.0	$4.67E^{-02}$	0.6
4.51	$C_{27}H_{30}O_{15}$	Kaempferol-3-*O*-rutinoside	Flavonols	4.6	$1.43E^{-02}$	1.8	3.5	$2.50E^{-02}$	2.1	2.9	$1.67E^{-02}$	1.8
5.03	$C_{24}H_{22}O_{13}$	Malonyl-genistin*	Isoflavones	1.4	$3.93E^{-02}$	2.4	––	––	––	––	––	––
6.30	$C_{18}H_{32}O_5$	Trihydroxy-octadecadienoic acid	Fatty acids	1.3	$4.64E^{-02}$	1.3	1.3	$4.58E^{-02}$	1.9	1.3	$4.33E^{-02}$	1.4
6.49	$C_{15}H_{10}O_5$	Genistein*	Isoflavones	1.6	$2.86E^{-02}$	3.0	––	––	––	––	––	––
6.61	$C_{48}H_{78}O_{19}$	Soyasaponin Ba (V)	Triterpenoid saponins	1.4	$2.14E^{-02}$	1.2	––	––	––	3.4	$3.67E^{-02}$	1.1
8.70	$C_{48}H_{86}O_{18}P_2$	Phosphoinositide phosphate	Glycerophosphoinositol phosphates	––	––	––	2.4	$2.92E^{-02}$	1.4	2.5	$2.33E^{-02}$	1.3
9.57	$C_{48}H_{74}O_{17}$	Soyasaponin *γ*g	Triterpenoid saponins	––	––	––	––	––	––	3.9	$3.00E^{-02}$	1.5
9.90	$C_{45}H_{74}O_{11}$	Monogalactosyldiacylglycerol (18:3)	Monogalactosyldiacylglycerols	2.8	$2.50E^{-02}$	2.1	8.7	$1.67E^{-02}$	4.1	6.1	$6.67E^{-03}$	3.7
10.15	$C_{31}H_{58}O_{14}$	Lyso-monogalactosyldiacylglycerols (16:0/0:0)	Lyso-monogalactosyldiacylglycerols	––	––	––	2.2	$2.08E^{-02}$	1.9	3.3	$1.00E^{-02}$	2.7
11.74	$C_{22}H_{43}O_9P$	Phosphatidylglycerol (16:1 (9Z)/0:0)	Phosphatidylglycerols	1.9	$3.21E^{-02}$	1.8	––	––	––	2.2	$2.00E^{-02}$	2.4
11.90	$C_{41}H_{66}O_{13}$	Soyasaponin Bc' (IV)	Triterpenoid saponins	2.1	$3.57E^{-02}$	1.2	2.0	$3.75E^{-02}$	1.5	3.4	$1.33E^{-02}$	1.8
13.64	$C_{46}H_{75}O_{10}P$	Phosphatidylglycerol (18:2/22:6)	Phosphatidylglycerols	––	––	––	––	––	––	2.9	$2.67E^{-02}$	2.0

Metabolites were annotated by level 2.1 of the metabolomics standards initiative; t_R – retention time; KVL – very low K^+ availability; KVH – very high K^+ availability; LT – lower third; MT – medium third; UT– upper third; "*" - identified using authentic standards; "–" - not significant; O2PLS-DA and S-Plot models were performed using p-value ≤ 0.05 and false discovery rate (FDR) with q-value ≤ 0.05 (Data S1); Importance variable in score projection (VIP ≥ 1.0) were considered; Fold change (FC) refers to metabolite relative intensity values between KVH *vs.* KVL treatments (metabolite content is higher in KVH than KVL treatment); MS^1 and MS^2 data, chemical ontology and KEGG Pathway are available in Supplementary Data 1.

Table 5
Putative metabolite identification from soybean pod tissues upregulated under very high potassium (KVH) availability by UPLC-QTof-MS^E.

t_R (min)	Formula	Identification	Chemical Ontology	FC	FDR	VIP
		Immature Seeds				
6.33	$C_{18}H_{32}O_5$	Trihydroxy-octadecadienoic acid	Fatty acids	2.7	$4.58E^{-02}$	1.7
8.61	$C_{42}H_{68}O_{14}$	Soyasaponin Bb' (III)	Triterpenoid saponins	1.8	$8.33E^{-03}$	1.9
		Pod Valves				
0.70	$C_6H_8O_7$	Citric acid	Tricarboxylic acids	1.6	$2.00E^{-02}$	1.1
0.70	$C_4H_4N_2O_2$	Uracil	Pyrimidones	1.5	$4.00E^{-02}$	2.2
2.79	$C_{18}H_{28}O_9$	β-D-glucopyranosyl-11-hydroxyjasmonic acid	Fatty acyl glycosides	1.7	$3.33E^{-03}$	1.3
3.86	$C_{27}H_{30}O_{16}$	Kampferol-3-*O*-digalactopyranoside	Flavonols	1.5	$4.33E^{-02}$	1.8
5.00	$C_{24}H_{22}O_{13}$	Malonyl-genistin*	Isoflavone	1.5	$4.67E^{-02}$	2.3

Metabolites were annotated by level 2.1 of the metabolomics standards initiative; t_R – retention time; KVL – very low K^+ availability; KVH – very high K^+ availability; "*" – identified using authentic standards; O2PLS-DA and S-Plot models were performed using p-value ≤ 0.05 and false discovery rate (FDR) with q-value ≤ 0.05 (Data S1); Importance variable in score projection (VIP ≥ 1.0) were considered; Fold change (FC) refers to metabolite relative intensity values between KVH *vs.* KVL treatments (metabolite content is higher in KVH than KVL treatment); MS^1 and MS^2 data, chemical ontology and KEGG Pathway are available in Supplementary Data 1.

and membrane lipids. Additionally, nine terpenoids were putatively identified as sesquiterpenoid and triterpenoid saponins, and seven were carbohydrates; besides of eleven compounds classified as organic acids, amino acids, and nucleic acids (Data S1).

Fifty-one annotated metabolites of soybean plants influenced by contrasting soil potassium availability were correlated using the KEGG database. These compounds were linked to nineteen metabolic pathways, such as alanine, aspartate, glutamate, histidine, *β*-alanine, citrate cycle, glyoxylate and glucuronate interconversion, nitrogen, galactolipid, glycerophospholipid, α-linolenic acid, purine and pyrimidine metabolism, arginine, aminoacyl-tRNA, galactosylcyclitol, phenylpropanoid, flavonol, isoflavonoid, sesquiterpenoid, and triterpenoid biosynthesis. Overall, these KEGG pathways belong to the pathway maps that include carbohydrates, amino acids, nucleotides, lipids, specialised metabolites, and energetic metabolism (Data S1).

2.6. Soybean leaves under K^+ homeostasis

Flavonol glycosides, as kaempferol 3-glucosyl-(1 → 2)-gentiobioside, kaempferol-3-*O*-*α*-L-rhamnopyranosyl-(1 → 6)-*β*-D-galactopyranoside, and kaempferol-3-*O*-rutinoside were upregulated in soybean leaves of fertilised plants (KVH) when compared to very low potassium availability (KVL) treatment (Table 4). Flavanols are usually associated with pathogen, insect resistance (Dillon et al., 2017), and protection from UV-B effects (Harborne and Williams, 2000). Previous studies also reported that K^+ nutrition provoked an increase in phenolic compounds, as ferulic, cinnamic, salicylic, and rosmarinic acids (Gao et al., 2018; Nguyen et al., 2010; Prasad et al., 2010). In fact, K^+ favours metabolic

Table 6
Putative metabolite identification from soybean leaves upregulated under very low potassium (KVL) availability by UPLC-QTof-MS^E.

t_R (min)	Formula	Identification	Chemical Ontology	Lower Third (LT)			Medium Third (MT)			Upper Third (UT)		
				KVH-LT *vs.* KVL-LT			KVH-MT *vs.* KVL-MT			KVH-UT *vs.* KVL-UT		
				FC	FDR	VIP	FC	FDR	VIP	FC	FDR	VIP
0.64	$C_4H_8N_2O_3$	L-asparagine	Amino acids	––	––	––	8.0	$2.31E^{-02}$	1.0	16.6	$3.57E^{-03}$	1.8
0.68	$C_4H_8N_4O_4$	Allantoic acid	Amino acids	––	––	––	––	––	––	3.3	$2.86E^{-02}$	1.3
0.71	$C_4H_4N_2O_2$	Uracil	Pyrimidones	3.1	$3.33E^{-03}$	1.7	2.1	$3.85E^{-03}$	1.7	2.4	$1.07E^{-02}$	1.6
0.72	$C_6H_8O_7$	Citric acid	Tricarboxylic acids	2.4	$6.67E^{-03}$	2.6	1.7	$7.69E^{-03}$	2.6	2.0	$7.14E^{-03}$	2.7
1.60	$C_{13}H_{16}O_9$	Gentisic acid 2-*β*-*D*-glucoside	Benzoic acids	1.3	$4.67E^{-02}$	1.0	2.6	$1.15E^{-02}$	2.6	3.0	$1.79E^{-02}$	2.3
4.60	$C_{21}H_{20}O_{10}$	Genistin*	Isoflavones	––	––	––	1.2	$5.00E^{-02}$	1.9	1.5	$1.43E^{-02}$	3.7
5.03	$C_{24}H_{22}O_{13}$	Malonyl-genistin*	Isoflavones	––	––	––	1.6	$3.85E^{-02}$	2.6	2.9	$3.21E^{-02}$	3.1
5.14	$C_{23}H_{22}O_{11}$	Acetyl-genistin*	Isoflavones	––	––	––	1.6	$3.08E^{-02}$	1.3	2.5	$3.57E^{-02}$	1.2
5.47	$C_{15}H_{10}O_4$	Daidzein*	Isoflavones	2.7	$5.00E^{-02}$	1.0	––	––	––	16.1	$4.64E^{-02}$	1.1
6.49	$C_{15}H_{10}O_5$	Genistein*	Isoflavones	––	––	––	––	––	––	1.3	$5.00E^{-02}$	2.4
6.51	$C_{16}H_{10}O_6$	Isotrifoliol	Coumestans	2.1	$4.00E^{-02}$	1.4	––	––	––	ND	ND	ND
6.61	$C_{15}H_8O_5$	Coumestrol	Coumestans	2.4	$3.67E^{-02}$	4.5	––	––	––	––	––	––
7.04	$C_{16}H_{10}O_6$	Trifoliol	Coumestans	3.5	$3.33E^{-02}$	2.3	––	––	––	ND	––	ND
8.15	$C_{20}H_{16}O_6$	Unknown	Unknown	9.2	$2.00E^{-02}$	1.5	––	––	––	ND	––	ND
8.40	$C_{51}H_{80}O_{21}$	Malonyl-dHex-Hex-HexA-soyasapogenol B (Pisumsaponin I)	Triterpenoid saponins	––	––	––	1.8	$2.69E^{-02}$	1.1	2.6	$2.50E^{-02}$	1.5
8.50	$C_{48}H_{76}O_{18}$	Soyasaponin Be (Dehydrosoyasaponin I)	Triterpenoid saponins	––	––	––	2.1	$1.54E^{-02}$	1.0	2.6	$2.14E^{-02}$	1.3
8.52	$C_{21}H_{22}O_5$	Glyceollin IV	Pterocarpans	7.0	$2.67E^{-02}$	1.3	––	––	––	––	––	––
8.95	$C_{20}H_{16}O_5$	Phaseol (4-prenyl-coumestrol)	Coumestans	3.4	$2.33E^{-02}$	5.2	––	––	––	––	––	––
8.98	$C_{53}H_{82}O_{20}$	Soyasaponin *β*a	Triterpenoid saponins	4.9	$1.33E^{-02}$	2.2	2.9	$3.46E^{-02}$	2.4	2.3	$3.93E^{-02}$	2.1
9.11	$C_{54}H_{84}O_{21}$	Soyasaponin *β*g	Triterpenoid saponins	4.7	$1.00E^{-02}$	2.1	3.0	$1.92E^{-02}$	2.3	2.0	$4.29E^{-02}$	1.8
12.47	$C_{22}H_{45}O_9P$	Phosphatidylglycerol (16:0/0:0)	Phosphatidylglycerols	4.8	$1.67E^{-02}$	1.2	––	––	––	––	––	––

Metabolites were annotated by level 2.1 of the metabolomics standards initiative; t_R – retention time; KVL – very low K^+ availability; KVH – very high K^+ availability; LT – lower third; MT – medium third; UT– upper third; "*" – identified using authentic standards; "–" - not significant; "ND" – not detected; O2PLS-DA and S-Plot models were performed using p-value ≤ 0.05 and false discovery rate (FDR) with q-value ≤ 0.05 (Data S1); Importance variable in score projection (VIP ≥ 1.0) were considered; Fold change (FC) refers to metabolite relative intensity values between KVL *vs.* KVH treatments (metabolite content is higher in KVL than KVH treatment); MS^1 and MS^2 data, chemical ontology and KEGG Pathway are available in Supplementary Data 1.

Table 7
Putative metabolite identification from soybean pod tissues upregulated under very low potassium (KVH) availability by UPLC-QTof-MS^E.

t_R (min)	Formula	Identification	Chemical Ontology	FC	FDR	VIP
		Immature Seeds				
0.62	$C_6H_9N_3O_2$	L-histidine	Amino acids	1.8	$2.50E^{-02}$	2.4
0.64	$C_5H_{10}N_2O_3$	L-glutamine	Amino acids	2.4	$3.33E^{-02}$	1.4
0.65	$C_4H_8N_2O_3$	L-asparagine	Amino acids	1.6	$4.17E^{-02}$	1.8
0.66	$C_{18}H_{32}O_{15}$	Oligosaccharide unknown	Oligosaccharides	2.8	$2.92E^{-02}$	2.3
0.66	$C_{17}H_{30}O_{15}$	Oligosaccharide unknown	Oligosaccharides	2.1	$3.75E^{-02}$	1.8
0.67	$C_6H_{12}O_7$	Galactonic acid	Hydroxy acids	3.9	$1.25E^{-02}$	1.8
0.67	$C_{19}H_{34}O_{16}$	Ciceritol	Oligosaccharides	1.7	$5.00E^{-02}$	1.3
0.69	$C_{19}H_{20}O_{12}$	3,5-dihydroxyphenyl 1-*O*-(6-*O*-galloyl-*β*-D-glucopyranoside)	Oligosaccharides	1.6	$1.67E^{-02}$	4.0
5.41	$C_{15}H_{10}O_4$	Daidzein*	Isoflavones	1.5	$2.08E^{-02}$	2.4
6.50	$C_{15}H_{10}O_5$	Genistein*	Isoflavones	17.8	$4.17E^{-03}$	2.8
		Pod Valves				
0.64	$C_5H_{10}N_2O_3$	L-glutamine	Amino acids	2.1	$2.67E^{-02}$	1.1
0.65	$C_4H_8N_2O_3$	L-asparagine	Amino acids	2.4	$1.33E^{-02}$	2.1
0.66	$C_{11}H_{20}O_{10}$	3-*O*-*β*-D-galactopyranosyl-L-arabinose	Monosaccharides	2.9	$1.67E^{-02}$	1.3
0.68	$C_3H_7N_3O_3$	Ureidoglycine	Amino acids	1.9	$3.67E^{-02}$	2.0
0.69	$C_4H_8N_4O_4$	Allantoic acid	Amino acids	1.6	$2.33E^{-02}$	2.0
0.73	$C_4H_6O_5$	Malic acid	Beta hydroxy acids	2.2	$5.00E^{-02}$	1.2
0.74	$C_{13}H_{16}O_9$	Gentisic acid 2-*β*-D-glucoside	Benzoic acids	2.1	$6.67E^{-03}$	1.4
1.62	$C_{13}H_{16}O_9$	Protocatechuic acid 4-*O*-*β*-glucoside	Benzoic acids	1.4	$3.00E^{-02}$	1.5
2.34	$C_{21}H_{32}O_{10}$	Dihydrophaseic acid 4-*O*-*β*-D-glucoside	Sesquiterpenoids	1.6	$1.00E^{-02}$	2.3
3.64	$C_{21}H_{20}O_9$	Daidzin*	Isoflavones	2.3	$3.33E^{-02}$	1.3

Metabolites were annotated by level 2.1 of the metabolomics standards initiative; t_R – retention time; KVL – very low K^+ availability; KVH – very high K^+ availability; "*" – identified using authentic standards; O2PLS-DA and S-Plot models were performed using p-value ≤ 0.05 and false discovery rate (FDR) with q-value ≤ 0.05 (Data S1); Importance variable in score projection (VIP ≥ 1.0) were considered; Fold change (FC) refers to metabolite relative intensity values between KVL *vs.* KVH treatments (metabolite content is higher in KVL than KVH treatment); MS^1 and MS^2 data, chemical ontology and KEGG Pathway are available in Supplementary Data 1.

reactions and the cells turgidity, maintaining the leaves orientation for major light interception (Malavolta, 1980), suggesting the differential regulation of phenolic compounds can be associated with UV-B.

Monogalactosyldiacylglycerol (18:3) and lyso-monogalactosyl diacylglycerol (16:0/0:0) content also were upregulated (6.1- and 3.3-fold, respectively) in leaves of upper third, when soybean plants grown under KVH compared to KVL treatment (Table 4). In rice, galactolipid biosynthesis was downregulated in seedlings deprived of potassium nutrition, as reported by Shankar et al. (2013). Monogalactosyldiacylglycerol (MGDG) and digalactosyldiacylglycerol (DGDG) are major galactolipids constituents of chloroplast photosynthetic membranes (Murakawa et al., 2014); thus, the deficiency of these metabolites can be associated with impaired photosynthesis and plant light sensitivity (Jarvis et al., 2000).

Soyasaponins can occur constitutively in any soybean tissues (Tsuno et al., 2018; Yates et al., 2021). In our analyses, soybean plants under

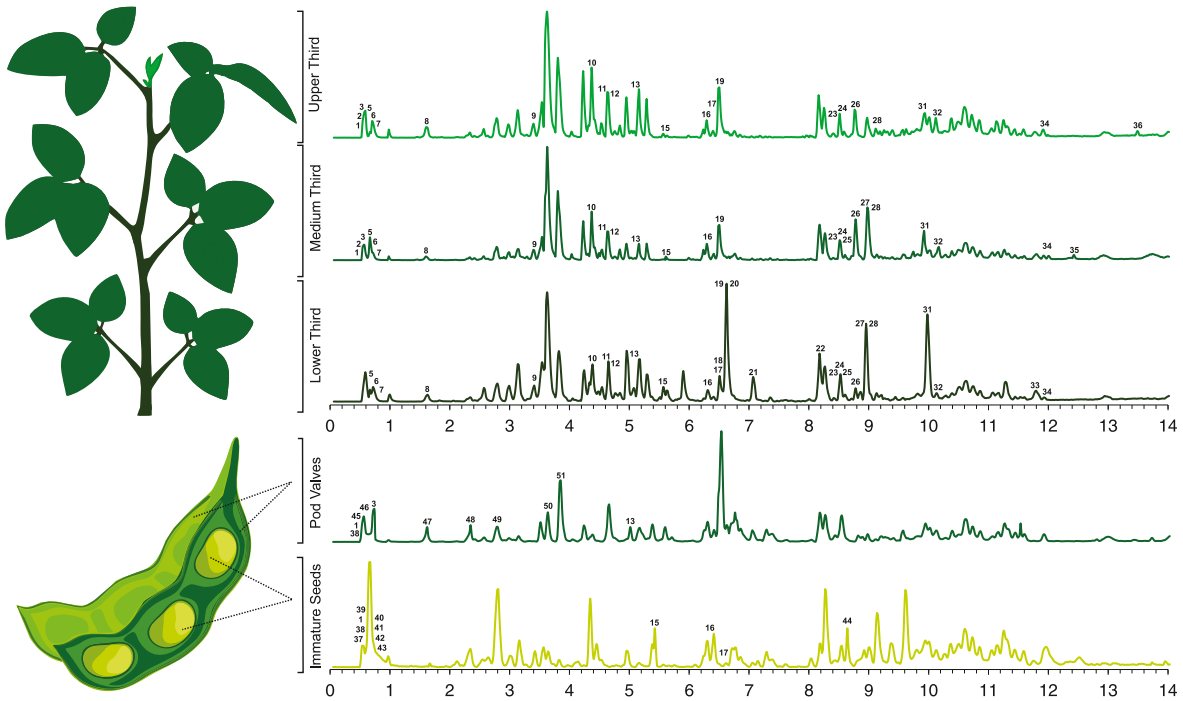

Fig. 2. Soybean tissues representation and base peak intensity (BPI) mass chromatograms (UPLC-QToF-MS^E) in negative ion mode (ESI$^-$) displaying comparative metabolomic profile differences. The corresponding list of metabolites annotated in the chromatograms is available in Supplementary Data 1.

potassium homeostasis (KVH) showed differential regulation (upregulation) of three triterpenoid saponins, as soyasaponin Ba (3.4-fold), soyasaponin γg (3.9-fold), and soyasaponin Bc′ (3.4-fold) in the UT leaves (Table 4). Nevertheless, soybean leaves under very low potassium availability (KVL) also showed upregulation of four additional soyasaponins. Soyasaponin Bc′ and soyasaponin γg have the same structure, except for the conjugate 2,3-dihydro-2,5-dihydroxy-6-methyl-4*H*-pyran-4-one (DDMP) moiety. Upregulation of soyasaponin γg and soyasaponin Bc′ biosynthesis (>3.3-fold) were also detected after abiotic stress, as occurred in common bean seed of plants grown under severe drought condition (Herrera et al., 2019). Shankar et al. (2013) revealed that when K^+ privation is imposed on the rice seedlings, gene expression of terpenoid biosynthesis is reduced. Moreover, other macronutrients, such as nitrogen and phosphate availability can alter saponin content (Szakiel et al., 2011).

2.7. Soybean pod tissues under K^+ homeostasis

Metabolomics analysis of pod tissues showed increased concentration of kaempferol-3-*O*-digalactopyranoside (1.5-fold), malonyl-genistin (1.5-fold), *β*-D-glucopyranosyl-11-hydroxyjasmonic acid (1.7-fold), trihydroxy-octadecadienoic acid (2.7-fold), and soyasaponin Bb′ (1.8-fold) in plants grown under KVH in contrast with KVL treatment (Table 5). Isoflavone content increases in soybean seeds when plants are grown under K^+ rates were reported by Bellaloui et al. (2013) and Vyn et al. (2002). Especially, Seguin and Zheng (2006) described the difference in isoflavonoid content was not significant when K^+ was applied in medium-to high-fertility soils. In fact, we expected that the upregulation of flavonoids and isoflavones, in our trial caused by K^+ fertilization, would be higher in immature seed extracts. Nevertheless, it is necessary to consider that this regulation is also dependent on yearly environmental factors (drought and temperature), edaphic conditions, and potassium soil content.

2.8. Soybean leaves under K^+ deficiency

The metabolomic profile of leaf samples from plants grown in KVL showed differential regulation at 21 metabolites, compared to KVH (Table 6). Under potassium deficiency, soybean leaves revealed upregulation of amino acids, benzoic acid derivatives, pyrimidines, tricarboxylic acids, isoflavones, coumestans, pterocarpans, phosphatidylglycerols, and triterpenoid saponins content. The phytoalexins (isoflavonoids and soyasaponins) were the major class of specialised metabolites elicited in K^+ deficient soybean leaves (Table 6 and Fig. 4).

The amino acids mostly accumulated in UT trifoliate leaves of plants in KVL were allantoic acid (3.3-fold) and L-asparagine (16.6-fold) compared to KVH treatment (Table 6). L-asparagine was also a differentially regulated metabolite in PV (2.4-fold) and IS (1.6-fold) in KVL treatment (Table 6 and Table 7). Both metabolites are participants in soybean nitrogen metabolism (alanine, aspartate, glutamate, and purine metabolism) by KEGG Metabolic Pathway (Data S1). Previously, L-asparagine was differentially regulated in Fabaceae plants under potassium deficiency (Stewart and Larher, 1980). L-asparaginases (EC 3.5.1.1) have been associated with K^+ dependence for catalytic activity, promoting L-asparagine hydrolysis in L-aspartate and ammonium (Bruneau et al., 2006; Lea et al., 2007). However, changes in the content of L-asparagine can favour pest infestation, as *Aphis glycines* in soybean (Severtson et al., 2016; Walter and DiFonzo, 2007) and *Myzus persicae* in *Brassica napus* (Severtson et al., 2016). Therefore, based on previous studies (Amtmann et al., 2008; Walter and DiFonzo, 2007) and our results, we consider that L-asparagine and other amino acids changes can affect soybean pest infestation and such susceptibility is an important issue for future research.

Four soyasaponins were upregulated in leaves from plants under very low potassium availability (KVL), as malonyl-dHex-Hex-HexA-soyasapogenol B (≤ 2.6-fold), soyasaponin Be (≤ 2.6-fold), soyasaponin *β*a (≤ 4.9-fold), and soyasaponin *β*g (≤ 4.7-fold). However, the regulation of soyasaponin Be and malonyl-dHex-Hex-HexA-soyasapogenol was restricted to MT and UT leaves, being undetectable in the LT (Table 6). Interestingly, the soyasaponins elicited in plants under deficiency were heterosides containing soyasapogenol B (aglycone) plus three moiety units conjugated to position C-3. Soyasaponin *β*a and soyasaponin *β*g have a DDMP moiety and pisumsaponin I, a malonyl

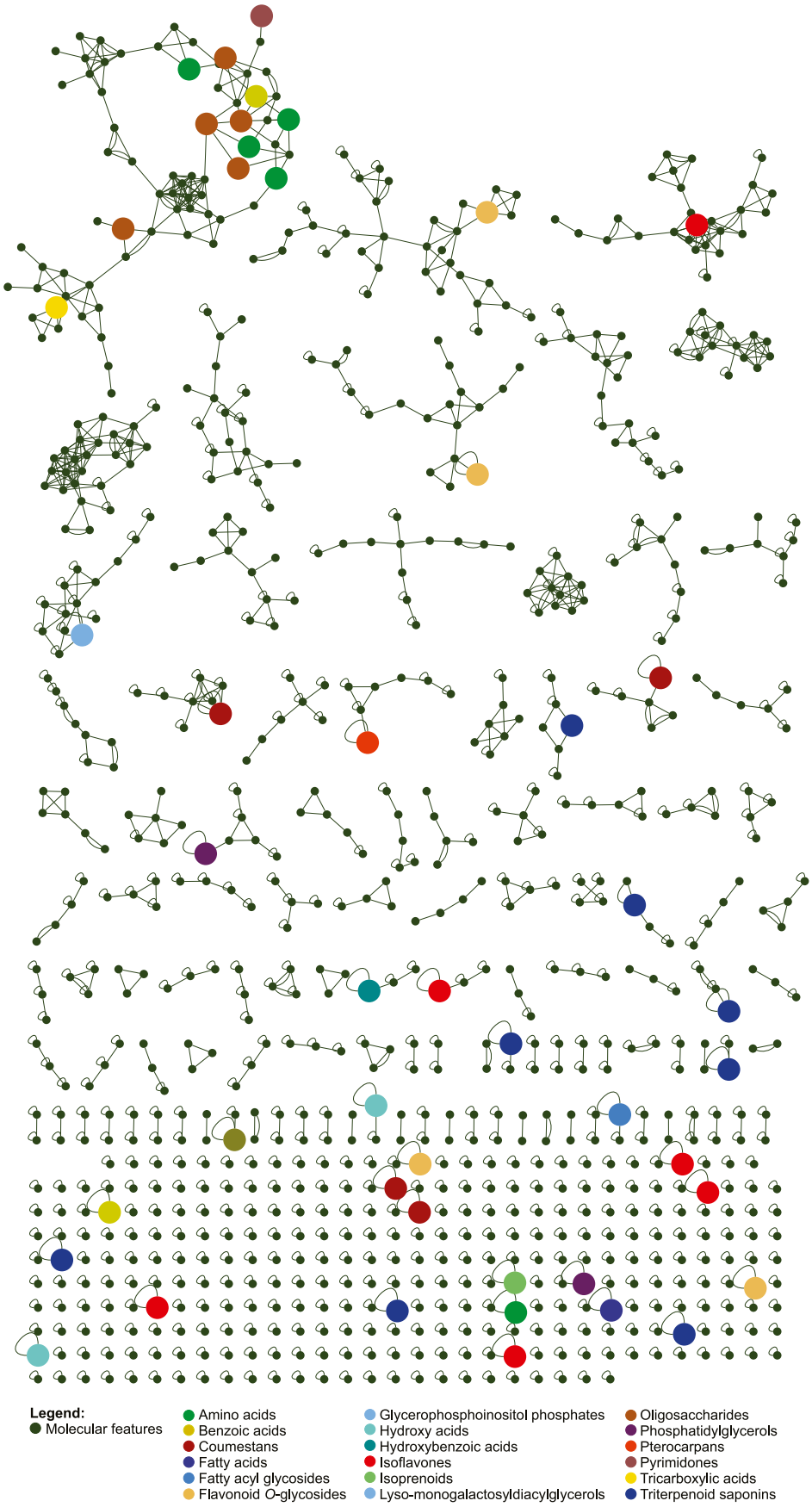

Fig. 3. Complete feature-based molecular network (FBMN) in global natural product social molecular networking (GNPS) of soybean trifoliate leaves and pod tissues, influenced by K^+ availability. Nodes represent MS^2 spectra and are connected based on spectral similarity defined (cosine score $\geq$ 0.8), matched fragment ion (5), and network TopK (10), encompassing 902 nodes and 1430 edges organised in 89 spectral molecular families. Large coloured nodes represent metabolites influenced by K^+ nutrition identified by chemometrics models and representative chemical ontology.

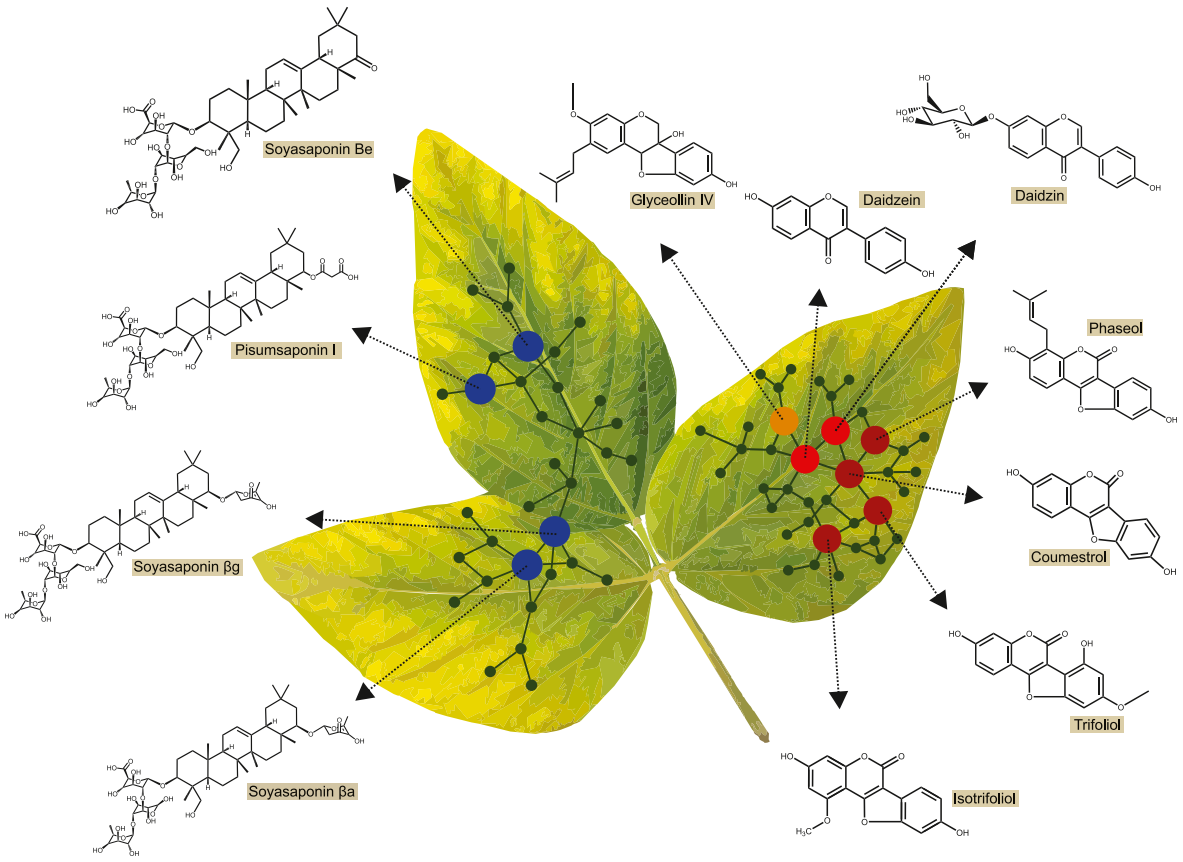

Fig. 4. Isoflavonoids (isoflavones, coumestans and pterocarpans) and triterpenoid saponins (soyasaponins) as phytoalexins upregulated in soybean leaves under very low potassium availability.

group, both in the C-22 hydroxyl position. DDMP-conjugated saponins showed pro-oxidative and superoxide radical ($O_2^{\cdot-}$) scavenging activity, and this property was attributed to the DDMP moiety (Okubo and Yoshiki, 2000; Yoshiki and Okubo, 1995). DDMP saponins accumulation in K^+ deficient plants can be associated with oxygen radical controllers in soybean leaves under oxidative stress (Yoshiki et al., 1998).

Isoflavonoids (isoflavones, coumestans, and pterocarpans) were predominantly upregulated compounds in soybean plants under KVL treatment (Table 6). The isoflavonoids have been frequently detected in soybean leaves (Hoffmann-Campo et al., 2001; Piubelli et al., 2005) and pods (da Graça et al., 2016; Piubelli et al., 2005) under biotic interactions. This class of flavonoid can be observed, as constitutive (phytoanticipins) or induced (phytoalexins) metabolites (Graham et al., 1990; Simons et al., 2011; Tiku, 2020). Our results indicated upregulation of isoflavones genistein (1.3-fold), malonyl-genistin ($\leq$ 2.9-fold), acetyl-genistein ($\leq$ 2.5-fold), and daidzein ($\leq$ 16.1) in leaves of plants under K^+ soil deficiency (Table 6). Chemometrics models showed that glycosylated isoflavones were predominantly accumulated in leaf extracts from medium (MT) and upper third (UT) of soybean plants. The biosynthesis of aglycone daidzein in LT leaves was 2.7-fold upregulated in KVL compared with KVH. Interestingly, the differential regulation of this compound was 16.1-fold greater in UT, and no changes were detected in MT leaves. These experimental results suggested the LT leaves primarily had to cope with potassium deficiency at V7 stage, when soybean samples were collected. Potassium is a highly mobile nutrient in the plant; its redistribution was therefore expected and revealed by the ionomic analysis. In addition, although different tissues had different metabolites depending on the tissue maturity, they are part of the same organism that has complex and induced responses. The high daidzein upregulation in upper third (UT) leaves can be associated with induced mechanisms. This condition suggests that UT leaves were preparing to deal with the stress caused by K^+ lacking, a situation that already occurred in the older leaves. Furthermore, our results demonstrated that K^+ deficiency accumulated not only the aglycones but also glycosidic isoflavones, corroborating previous investigations after stress by herbicide acifluorfen (Cosio et al., 1985), ethylene application (Ban et al., 2020), *Nezara viridula* (Piubelli et al., 2003) and *Spodoptera litura* herbivory (Murakami et al., 2014).

Leaves under very low K^+ availability (KVL) showed a higher daidzein content that was exclusively differently regulated under stress (KVL *vs.* KVH). This aglycone is a direct precursor of soybean phytoalexin biosynthesis, as coumestans and pterocarpans (Graham et al., 1990; Kuc, 1995). Chemometrics models revealed that leaves under nutritional stress upregulated biosynthesis of coumestans, as coumestrol (2.4-fold), isotrifoliol (2.1-fold), trifoliol (3.5-fold), phaseol (3.4-fold), as well as, gliceollin IV (7.0-fold) a pterocarpan (Table 6). The upregulation of these phytoalexins is likely associated with metabolism disorders and plant oxidative stress status (Ahmad et al., 2014; Hernandez et al., 2012). Our results suggest that this also occurs in soybean leaves under severe K^+ deficiency. Phytoalexins can be autotoxic to cells, therefore, upregulation of biosynthesis is generally associated with defence mechanisms. Previously, coumestans elicitation occur when *Phaseolus vulgaris* leaves were injured by sulphur dioxide, ozone, and herbicides (Rubin et al., 1983). Ozone fumigation, a highly reactive and cytotoxic agent, increased daidzein and coumestan contents in soybean (Keen and Taylor, 1975). Phaseol and other prenylated isoflavones were also detected in soybean cotyledons after lactofen (diphenyl ether) treatment (Cheng et al., 2011).

Previously published works were consistent in associating that potassium deficiency leads to status for the uncontrolled generation of reactive oxygen species (ROS) in plants (Ahmad et al., 2014; Cakmak, 2005; Hernandez et al., 2012; Miao et al., 2010). ROS are mainly

produced in chloroplasts and peroxisomes (Asada, 2000; Pospíšil, 2016) when plants are exposed to nutrient deficiency, salinity, and water deficit (Cakmak, 1994; Foyer et al., 1994). Interestingly, ROS generation is enhanced when plants are under abiotic stress and also exposed to light, causing photo-oxidative damage to chloroplasts (Cakmak and Marschner, 1992; Issawi et al., 2018; Marschner and Cakmak, 1989), and photodynamic stress status (Issawi et al., 2018). Under low K^+ availability and sufficient contents of other nutrients, plants usually showed chlorotic and necrotic tissues when exposed to light (Cakmak, 2005; Marschner et al., 1996). However, these symptoms were absent when plants were maintained under shading (Marschner and Cakmak, 1989). Phosphorus and iron deficiency typically cause chlorotic symptoms (Marschner, 2012). Nevertheless, in our experiment, independently of K^+ availability, phosphorus content remained unaltered, and iron content increased in leaves severely K^+ deficient, supporting our findings that leaf symptoms were only associated with K^+ deficiency.

The metabolomic profile of soybean plants under potassium deficiency showed differential regulation of DDMP saponins that are oxygen radical controllers in *G. max* (Yoshiki et al., 1998). Isoflavones and pterocarpans (e.g., daidzein, isotrifoliol, and phaseol) are excellent free radical inhibitors and lipid oxidation reductors (Boué et al., 2008; Lee et al., 2005; Li et al., 2017; Toda and Shirataki, 1999). Based on previous works and our results, we suggested that soybean metabolism was reprogrammed for the biosynthesis of non-constitutive specialised metabolites (phytoalexins) for handling oxidative damage caused by potassium starvation.

2.9. Soybean pod tissues under K^+ deficiency

Eighteen metabolites were differentially regulated in K^+ deficient soybean pod tissues (Table 7). Unlike in leaves, amino acids were the main class of metabolites differentially regulated in the pod tissues. L-glutamine and L-asparagine were upregulated (≤2.4-fold) in immature seeds (IS) and pod valves (PV), and the amino acids belonging to the nitrogen metabolism pathway, as ureidoglycine (1.9-fold in PV) and allantoic acid (1.6-fold in PV) were not differentially regulated in IS.

Metabolomic profile analyses indicated positive regulation of the isoflavones daidzein (1.5-fold) and genistein (17.8-fold) in IS, and daidzin (2.3-fold) in PV tissues when plants grew under K^+ deficiency (Table 7). In our analysis, genistein is highly regulated in IS; the conjugated metabolite genistein (genistin) was also induced by the stink bug, *Nezara viridula*, whose damage (seed punctures) are directly imposed in seeds (Piubelli et al., 2003), but the concentration increases 3.1-fold. Additionally, higher upregulation of genistein was detected when soybean plants were under abiotic stress, such as salt stress, flooding, and shading (Liu et al., 2017; VanToai et al., 2012; Wu et al., 2008).

Low K^+ availability also showed upregulation of protocatechuic acid-4-*O*-*β*-glucoside (1.4-fold) and gentisic acid-5-*O*-*β*-glucoside (2.1-fold) in PV, and L-histidine (1.8-fold) only in IS (Table 7). Protocatechuic and gentisic acids (benzoic acids) are effective antioxidants and inhibitors of lipid peroxidation (Moran et al., 1997; Rice-Evans et al., 1997). Whereas, L-histidine is associated with energetic storage compounds, control of hydroxyl radicals (Zs-Nagy and Floyd, 1984), and singlet oxygen ($^1O_2$) (Wade and Tucker, 1998). Our results demonstrate that soybean pods and leaves (reproductive and vegetative structures) even with different compounds being regulated, many of them are considered antioxidants; therefore, the biosynthesis of these compounds must have similar purposes, such as a mechanism to control oxidative stress status in soybean plants under very low K^+ availability.

3. Conclusions

Untargeted metabolomics reveals 51 primary and specialised metabolites acting in 19 biochemical pathways that were influenced by K^+ availability. The biochemical mechanisms of soybeans in response to very low K^+ availability are associated to: (I) accumulation of Ca^{2+}, Mg^{2+}, Fe^{2+}, Cu^{2+}, and B in young and old leaves; (II) increase of Fe^{2+} and Cu^{2+} content in immature seeds and pod valves, respectively; (III) leaf metabolism reprogramming for the biosynthesis of phytoalexins, such as isoflavones, coumestans, pterocarpans, and soyasaponins; (IV) enhancement of the amino acids, mono and oligosaccharides, benzoic acid derivatives, and isoflavones content in soybean pods (IS and PV); (V) L-asparagine accumulation in vegetative (leaves) and reproductive (pod tissues) structures.

Overall, the results suggest that soybean metabolism reprogramming is associated with oxidative stress caused by low K^+ availability, and show an increased content of phytoalexins (antioxidant agents), as isoflavonoids and triterpenoid saponins. Additionally, results suggest that L-asparagine is a promising soybean biomarker under K^+ deficiency.

Our data reveals that increasing fertilization rates did not promote a substantial increase in the content of constitutive specialised metabolites in soybean. We understood that this interaction is more complex and thus further work using integrated omics is certainly required, to understand whether the profile of metabolites induced by biotic elicitors (e.g., insects or pathogens) may be associated to K^+ content in plants.

4. Experimental

4.1. General experimental procedures

Leucine-enkephalin (Waters Technologies, USA) and quercetin (≥ 95% HPLC, Sigma-Aldrich, USA) were used as external control standards. Formic acid LiChropur™ (98–100% HPLC, Merck, Germany), acetonitrile and methanol Chromasolv™ (≥ 99.9% LC-MS, Honeywell, Germany) were the solvents for running the samples in chromatographic analysis. Reference standards were applied to compare retention time, MS^1 and MS^2 data including, daidzin, genistin, glycitin, malonyl-daidzin, malonyl-genistin, malonyl-glycitin, acetyl-daidzin, acetyl-genistin, acetyl-glycitin, daidzein, genistein, glycitein, and coumestrol (≥ 95% HPLC; Sigma-Aldrich, USA). All aqueous solutions were prepared using a Milli-Q™ system-producing ultrapure water (18.2 MΩ cm^{-1}; Millipore, USA).

4.2. Experimental design and assay

The experiments were carried out at Embrapa Soybean Experimental Station (23°18′ 37″ S, 51°17′ 68″ W; 590 m asl) in Londrina, Paraná State, Brazil, set on a Rhodic Hapludox (Soil Survey Staff, 2014). This area has flat and smooth wavy topography, with 760 g kg^{-1} of clay in the no-tillage system (0–20 cm layer) of cultivation. The region has a humid subtropical climate (Cfa) according to the Köppen climate classification (Alvares et al., 2013). Four treatments expressing K^+ availability conditions were set: KVL (very low), KL (low), KM (medium), and KVH (very high), considering rates of 0, 40, 80, and 160 kg K_2O ha^{-1} $y\text{-}^1$, respectively. These rates were yearly (based on two or three cropping seasons per year), applied as potassium chloride - KCl (60% K_2O or 50% K). Subsequently, the soils at 0–0.2 m depth sites were randomly collected and homogenised to form a sample at each experimental unit in October 2019 using a soil auger (0.05 m diameter) (Table S1). The K^+ rates applied resulted in the four classes of K^+ soil content interpretation (KVL, KL, KM, and KVH) that were based on Pauletti and Motta (2019) for regional conditions (Paraná State, Brazil).

Seeds of *Glycine max* (L.) Merr. (Fabaceae) cv. BRS 1010 IPRO (VI maturity group) were sown on November 2nd, 2019, with a row spacing of 0.5 m and 15 seeds per linear metre, expecting a density of 300,000 plants ha^{-1}. The experimental design was a randomised block design, with plots of 4 m × 8 m, composed of four lines of 6 m, and six replicates. Before sowing, seeds were treated with cobalt (2 g ha^{-1}), molybdenum (20 g ha^{-1}) and inoculated with 2 mL kg^{-1} of *Bradyrhizobium japonicum* SEMIA 5079 (Oliveira Junior et al., 2020). Soil fertilization was carried out with 111 kg ha^{-1} of triple superphosphate - TSP (45% P_2O_5), as

recommended by Pauletti and Motta (2019).

4.3. Plant materials

Potassium is a very mobile nutrient in plants (Marschner, 2012); therefore, potential differences in leaf metabolomic profiles can vary according to tissue maturity. Thus, we sampled trifoliate leaves of soybean plants at the V7 stage (Fehr and Caviness, 1977) when in vegetative stage, the highest K^+ uptake occurs (Bender et al., 2015), and collected old and young leaves. Leaf samples were classified according to the growth region, lower third (LT), medium third (MT), and upper third (UT), and were collected 49 days after sowing (DAS), obtaining six replicates. Samples were immediately packed in liquid nitrogen. The fresh mass was measured on an AY220 Marte™ analytical balance (Shimadzu, Brazil) and stored at −80 °C in an ultrafreezer (Indrel Scientific, Brazil) at the Embrapa Chemical Ecology Laboratory. Subsequently, leaves were lyophilised at −55 °C for 48 h in an L101 freeze-dryer (Liotop, Brazil). Previous studies have associated potassium-deficient soils with the incidence of diseases caused by the pathogen *Cercospora kikuchii* in soybean pods (Meyer and Klepker, 2007; Seixas et al., 2020). Therefore, we also collected soybean pods (R5.5 stage) at 98 DAS, and immature seeds (IS) were detached from the valves (PV) and separately maintained at the same storage process previously described for the analysis of trifoliate leaves.

4.4. Soil chemical analysis

The collected soil samples were oven-dried at 45 °C for 48 h and sieved through a 2 mm. Extractable Ca^{2+}, Mg^{2+}, and Al^{3+} in 1 mol L^{-1} KCl (Mehlich, 1953) and plant-available P and K^+ were evaluated using Mehlich-1 solution (Mehlich, 1984). Soil pH was determined in 0.01 mol L^{-1} $CaCl_2$, and organic carbon (OC) following the procedures described by Walkley and Black (1934). The chemical attributes from the experimental area are available in Table S1.

4.5. Plant extraction

The plant material (soybean leaves, immature seeds, and pod valves) was ground in a mortar with liquid nitrogen for metabolomics and ionomics analyses. Ultra-performance liquid chromatography quadrupole-time-of-flight mass spectrometry (UPLC-QTof-MS^E) was used for metabolomics analysis at the Embrapa Chemical Ecology Laboratory. Plant ionomics was carried out in inductively coupled plasma optical emission spectroscopy (ICP-OES) at the Embrapa Plant and Soil Analysis Laboratory.

4.5.1. Extraction process for plant metabolomics

Metabolomic analysis was performed using a 90 mg aliquot of plant tissues in 15 mL Falcon tubes. For metabolite extraction, 3 mL of 80% methanol (MeOH: H_2O; 80:20; *v/v*) was added to the plant tissue. Subsequently, samples were placed in an LSUC2-500-22.5 (60 Hz frequency, 1300 W power; Logen Scientific, Brazil) ultrasonic bath for 20 min, vortexed for 10 s and centrifuged at 5500 rpm, at 4 °C for 20 min in a Sorvall™ Legend™ X1R centrifuge (Rotor 75,003,623; Thermo Fisher Scientific, USA). The supernatant (3 mL) was filtered with Millex-HV Durapore™ 0.45 μm Acrodisc Filter Syringes (SLHVX13NL, PVDF; Merck Millipore, Germany) into glass tubes for drying in N_2 flux in MA 4006 dry-block (400 W power; Marconi Equipamentos, Brazil). Samples were placed in a freezer at −20 °C until performing the analyses. For chromatographic analysis, samples were solubilised in 80% MeOH and filtered on Millex-HV Durapore™ 0.22 μm Acrodisc Filter Syringes (SLHVX13TL, PVDF; Merck Millipore, Germany), aiming at a final concentration of 2.5 mg mL^{-1}.

4.5.2. Extraction process for plant ionomics

Plant elemental content analysis was performed using a 150 mg aliquot of plant sample freeze-dried and ground in a mortar. Subsequently, the samples of plant tissue were digested in 6 mL nitric acid (HNO_3: H_2O; 50:50; *v/v*) and 2 mL hydrogen peroxide (H_2O_2) in a MARSXpress microwave oven (CEM Corporation, Canada). The conditions followed 10 min of the heating ramp, maintaining a constant temperature at 170 °C for 15 min under 2 MPa pressure and a power of 1600 W (USPEA, 1996).

4.6. Instrumental analyses

4.6.1. Chromatographic analysis (UPLC)

Chromatographic analyses were performed using ACQUITY UPLC™ ultra-performance liquid chromatography (Waters Corporation, USA) equipment set in a binary solvent system and sample manager. Aliquots (5 μL) of plant extracts were injected through an autosampler at 20 °C into an ACQUITY UPLC HSS C18 SB stationary reversed-phase column (100 mm × 2.1 mm; 1.8 μm; Waters Corporation, USA). The column temperature was maintained at 40 °C, with a flow rate of 0.4 mL min^{-1}. The mobile phase gradient was as follows: (A) binary elution system composed of Milli-Q™ ultrapure water and 0.1% formic acid (H_2O: CH_2O_2; *v/v*) and (B) acetonitrile with 0.1% formic acid (ACN: CH_2O_2; *v/v*). The gradient system was set 2–95% B (0–15 min), 100% B (15.1–17 min), and reconditioned with 2% B (17.1–19.1 min). Samples were injected in triplicate, randomly, and included blanks.

4.6.2. Mass spectrometry (ESI-QTof-MS^E)

A Xevo™ QTof-MS mass spectrometer (Waters Corporation, USA) equipped with a ZSpray™ source operating in negative electrospray ionization (ESI^-) was used for analyses. Data acquisition mass range was set at 100–1100 Da, and scan time at 0.25 s. MS Tune was configured for MS^E Centroid mode data acquisition, 6 V low collision energy on MS^1, and MS^2 function with ramp ranging from 20 to 40 V. The following MS parameters were applied in the analyses: 2.6 kV capillary voltage, 35 V sampling cone voltage, 150 °C supply temperature, and 1.5 V extraction cone voltage.

Nitrogen was produced by an NM30LA-MS high-purity N_2 generator (Peak Scientific Instrument™, Scotland), which was used as the cone gas, desolvation temperature, and flow at 350 °C and 500 L h^{-1}, respectively. Argon ≥ 99.9% purity (White Martins, Brazil) was used as collision gas at a pressure of 1.3 × 10^{-2} mbar. Mass accuracy and reproducibility were ensured by leucine-enkephalin infusion into the lock mass system (400 ng mL^{-1}), $[M-H]^-$ ion *m/z* 554.2615, and every 20 s on the LockSpray flow probe at 20 μL min^{-1}. The instrument was calibrated using a sodium formate standard solution and MassLynx™ 4.1 software (Waters Corporation, USA) used for data acquisition. Quercetin-3-*O*-rhamnoside was used as an external control standard (t_R = 5.64 min; *m/z* = $[M-H-Rha]^-$ 301.0348) analysed every 10 injections; the data of stability of UPLC-HRMS during the experiment was reported in Data S1.

4.6.3. Inductively coupled plasma (ICP-OES)

Plant tissue ionomics analyses were performed in an Optima™ 8300 ICP-OES (PerkinElmer, USA), and the macro and micronutrient contents were calculated using the calibration curve processed for each batch of samples (Table 1 and Table 2). In this workflow, we evaluated the profile of nutrients in soybean tissues under four soil nutrition conditions, very low (KVL; 0.05 $cmol_c$ dm^{-3}), low (KL; 0.09 $cmol_c$ dm^{-3}) medium (KM; 0.13 $cmol_c$ dm^{-3}) and very high (KVH; 0.50 $cmol_c$ dm^{-3}) K^+ availability by Mehlich-1 carried out after applying treatments (Table S1).

4.7. Yield parameters

At maturity soybean (R8 stage, 131 DAS), three rows of soybean 6 m in length were mechanically harvested to estimate the 100-seed dry weight (g) and soybean grain yield (kg ha^{-1}). The weight and moisture of the harvested seed were recorded, and the final seed yield was

calculated based on a standard method of seed moisture content of 130 g kg^{-1} (13%) water content (Table 3), as also described by Firmano et al. (2020).

4.8. Data interpretation

4.8.1. Univariate analysis

Yield parameters and ionomics data were submitted to analysis of variance (ANOVA), and means were compared using Tukey's test (p-value $\leq$ 0.05). Statistical comparisons between leaves from different growing regions (LT, MT, and UT) were performed using ANOVA + Tukey's test, and pod tissues (PV and IS) by two-sample t-test. ANOVA and Student's t-test were analysed in Minitab™ 18.1 software (Minitab Inc., USA)

4.8.2. Pre-processing and chemometrics analysis

Soybean leaf and pod extracts from K^+ treatments (KVL, KL, KM, and KVH) were analysed in a UPLC-QTof-MS^E system, and raw mass data were processed using MarkerLynx XS™ 4.1 software (Waters Corporation, USA). The processing parameters for chromatographic data were adjusted by retention time interval of 0–14 min. Mass acquisition amplitude was maintained from 100 to 1100 Da, mass tolerance was set at 0.04 Da, and the minimum peak intensity limit was considered at 50 counts. The isotopic data removal function was employed with smoothing (Savitzky-Golay); the noise elimination level was 9, and the window and mass retention times were set at 0.02 and 0.20, respectively. This procedure resulted in an LC-MS^1 dataset containing 625 features (t_R-m/z) from soybean extracts (leaves and pods). This dataset was imported into MarkerLynks XS for multivariate statistical analysis, which has an algorithm owned by Waters Corp. for non-detection of adducts.

Metabolomics (X) and ionomics (Y) analysis datasets, were submitted to multivariate analysis. Firstly, we employed the unsupervised model, based on principal component analysis PCA-X&Y, followed by the supervised model based on two-way orthogonal partial least squares discriminant analysis (O2PLS-DA). These chemometric tools help to reduce the dimension of the dataset and enable the visualization of variability sources. These models can join two multivariate matrices in a single model, allowing to visualize the interaction and variance of both datasets (X-variable: untargeted metabolomics analysis; Y-variable: targeted ionomics analysis). The supervised model parameters, based on O2PLS-DA, were evaluated from the R^2 values representing the model's explanatory capacity, while Q^2 suggested its predictive capacity (Table S6). The datasets resulting from O2PLS-DA became possible to compare the treatments KVL *vs*. KVH, and S-plot was performed for variable selection.

Potential markers were annotated based on four conditions: (I) selection of metabolites observed within the quadrant p(corr) [1] $\geq$ 0.6 and p[1] (loadings) $\geq$ 0.06 on the S-plot graph; (II) variable importance in projection (VIP) value $\geq$ 1 was used; (III) variables were selected when p-value $\leq$ 0.05 in the CV-ANOVA test; and (IV) false discovery rate (FDR), proposed by Benjamini and Hochberg (1995) was performed for calculating p-value transformation into q-value (Tugizimana et al., 2016; Vanderplanck and Glauser, 2018; Zhao et al., 2017; Zhu et al., 2018). Fold change was calculated by dividing the mean intensity values of metabolites in KVL *vs*. KVH treatments (Tables 4–7).

4.8.3. Metabolite annotation and molecular networking

Metabolomics data from the extracts analysed were imported into MS-DIAL 4.24 software (Tsugawa et al., 2015, 2019) for deconvolution and MS^E spectra alignment; posteriorly, putative identification was performed using MS-FINDER 3.44 (Tsugawa et al., 2016). Heuristic rules (Sumner et al., 2007) were considered, and the mass tolerance was adjusted to 0.02 Da. Metabolites were putatively identified according to metabolic standards initiative (MSI) of level 2.1 (Schrimpe-Rutledge et al., 2016; Sumner et al., 2007; Tsugawa et al., 2019), previously reported in *G. max* and botanical families based on the Human Metabolome Database (HMDB; https://hmdb.ca/), PubChem Database (https://pubchem.ncbi.nlm.nih.gov/), LipidMaps (LMSD; https://www.lipidmaps.org/), MassBank Database (https://mona.fiehnlab.ucdavis.edu/), ChemSpider (http://www.chemspider.com/), Kyoto Encyclopedia of Genes and Genomes Database (KEGG; https://www.genome.jp/kegg/compound/), Chemical Entities of Biological Interest (ChEBI; https://www.ebi.ac.uk/chebi/), FooDB (https://foodb.ca/), KnapSAcK (http://www.knapsackfamily.com/), and PlantCyc database (https://plantcyc.org/). A feature-based molecular networking (FBMN) workflow (Nothias et al., 2020) on global natural products social molecular networking (GNPS) (Wang et al., 2016) was created, and Cytoscape 3.8 (Shannon et al., 2003) using yFiled Layout Algorithms 1.1 and chemViz2 1.1 were used for network manipulation, visualization and analysis (Fig. 3). Chemical ontology descriptions, MS^2 fragments, average intensity, mass theoretical and measured data are available in Data S1.

Funding sources

This research was supported by the Brazilian Agricultural Research Corporation – Embrapa Soybean.

CRediT author statement

Gustavo dos Santos Cotrim: Conceptualization, Methodology, Formal Analysis, Investigation, Resources, Data curation, Writing – Original Draft, Writing – Review & Editing, Visualization. **Deivid Metzker da Silva**: Investigation, Writing – Review & Editing. **José Perez da Graça:** Investigation, Writing – Review & Editing. **Adilson de Oliveira Junior**: Conceptualization, Investigation, Resources, Writing – Review & Editing. **César de Castro**: Conceptualization, Investigation, Resources, Writing – Review & Editing. **Guilherme Julião Zocolo**: Writing – Review & Editing, Supervision. **Lucíola Santos Lannes**: Writing – Review & Editing, Supervision. **Clara Beatriz Hoffmann-Campo**: Conceptualization, Methodology, Resources, Writing – Review & Editing, Supervision, Project Administration, Funding Acquisition.

Declaration of competing interest

The authors declare that they have no known competing financial interests or personal relationships that could have appeared to influence the work reported in this paper.

Data availability

Data will be made available on request.

Acknowledgments

We thank Moisés de Aquino and Paulo Riceli Vasconcelos Ribeiro for technical assistance with the mass spectrometry analysis.

Appendix A. Supplementary data

Supplementary data to this article can be found online at https://doi.org/10.1016/j.phytochem.2022.113472.

References

Ahmad, P., Ashraf, M., Hakeem, K.R., Azooz, M., Rasool, S., Chandna, R., Akram, N.A., 2014. Potassium starvation-induced oxidative stress and antioxidant defense responses in *Brassica juncea*. J. Plant Interact. 9, 1–9. https://doi.org/10.1080/17429145.2012.747629.

Almeida, D.M., Oliveira, M.M., Saibo, N.J.M., 2017. Regulation of Na^+ and K^+ homeostasis in plants: towards improved salt stress tolerance in crop plants. Genet. Mol. Biol. 40, 326–345. https://doi.org/10.1590/1678-4685-gmb-2016-0106.

Alvares, C.A., Stape, J.L., Sentelhas, P.C., de Moraes Gonçalves, J.L., Sparovek, G., 2013. Köppen's climate classification map for Brazil. Meteorol. Z. 22, 711–728. https://doi.org/10.1127/0941-2948/2013/0507.

Amtmann, A., Rubio, F., 2012. Potassium in plants. In: eLS. John Wiley & Sons, Ltd, Chichester. https://doi.org/10.1002/9780470015902.a0023737.

Amtmann, A., Troufflard, S., Armengaud, P., 2008. The effect of potassium nutrition on pest and disease resistance in plants. Physiol. Plantarum 133, 682–691. https://doi.org/10.1111/j.1399-3054.2008.01075.x.

Armengaud, P., Sulpice, R., Miller, A.J., Stitt, M., Amtmann, A., Gibon, Y., 2009. Multilevel analysis of primary metabolism provides new insights into the role of potassium nutrition for glycolysis and nitrogen assimilation in *Arabidopsis* roots. Plant Physiol. 150, 772–785. https://doi.org/10.1104/pp.108.133629.

Asada, K., 2000. The water–water cycle as alternative photon and electron sinks. Phil. Trans. Roy. Soc. Lond. B Biol. Sci. 355, 1419–1431. https://doi.org/10.1098/rstb.2000.0703.

Ban, Y.J., Song, Y.H., Kim, J.Y., Baiseitova, A., Lee, K.W., Kim, K.D., Park, K.H., 2020. Comparative investigation on metabolites changes in soybean leaves by ethylene and activation of collagen synthesis. Ind. Crop. Prod. 154, 112743 https://doi.org/10.1016/j.indcrop.2020.112743.

Bellaloui, N., Yin, X., Mengistu, A., McClure, A.M., Tyler, D.D., Reddy, K.N., 2013. Soybean seed protein, oil, fatty acids, and isoflavones altered by potassium fertilizer rates in the Midsouth. Am. J. Plant Sci. 4, 976–988. https://doi.org/10.4236/ajps.2013.45121.

Bender, R.R., Haegele, J.W., Below, F.E., 2015. Nutrient uptake, partitioning, and remobilization in modern soybean varieties. Agron. J. 107, 563–573. https://doi.org/10.2134/agronj14.0435.

Benjamini, Y., Hochberg, Y., 1995. Controlling the false discovery rate: a practical and powerful approach to multiple testing. J. R. Stat. Soc. Ser. B 57, 289–300. https://doi.org/10.1111/j.2517-6161.1995.tb02031.x.

Boué, S.M., Shih, F.F., Shih, B.Y., Daigle, K.W., Carter-Wientjes, C.H., Cleveland, T.E., 2008. Effect of biotic elicitors on enrichment of antioxidant properties and induced isoflavones in soybean. J. Food Sci. 73, H43–H49. https://doi.org/10.1111/j.1750-3841.2008.00707.x.

Bruneau, L., Chapman, R., Marsolais, F., 2006. Co-occurrence of both L-asparaginase subtypes in *Arabidopsis*: at3g16150 encodes a K^+-dependent *L*-asparaginase. Planta 224, 668–679. https://doi.org/10.1007/s00425-006-0245-9.

Cakmak, I., Marschner, H., 1992. Magnesium deficiency and high light intensity enhance activities of superoxide dismutase, ascorbate peroxidase, and glutathione reductase in bean leaves. Plant Physiol. 98, 1222–1227. https://doi.org/10.1104/pp.98.4.1222.

Cakmak, I., 1994. Activity of ascorbate-dependent H_2O_2-scavenging enzymes and leaf chlorosis are enhanced in magnesium- and potassium-deficient leaves, but not in phosphorus-deficient leaves. J. Exp. Bot. 45, 1259–1266. https://doi.org/10.1093/jxb/45.9.1259.

Cakmak, I., 2005. The role of potassium in alleviating detrimental effects of abiotic stresses in plants. J. Plant Nutr. Soil Sci. 168, 521–530. https://doi.org/10.1002/jpln.200420485.

Castro, C. de, Oliveira Junior, A. de, Oliveira, F. A. de, Firmano, R.F., Zancanaro, L., Klepker, D., Foloni, J.S.S., Brighenti, A.M., Benites, V. de M., 2021. Magnesium: management for the nutritional balance of soybean, Documents 438. Embrapa Soybean, Londrina. ISSN 2176-2937.

Cheng, J., Yuan, C., Graham, T.L., 2011. Potential defense-related prenylated isoflavones in lactofen-induced soybean. Phytochemistry 72, 875–881. https://doi.org/10.1016/j.phytochem.2011.03.010.

Cosio, E.G., Weissenböck, G., McClure, J.W., 1985. Acifluorfen-induced isoflavonoids and enzymes of their biosynthesis in mature soybean leaves. Plant Physiol. 78, 14–19. https://doi.org/10.1104/pp.78.1.14.

Cui, J., Abadie, C., Carroll, A., Lamade, E., Tcherkez, G., 2019a. Responses to K deficiency and waterlogging interact via respiratory and nitrogen metabolism. Plant Cell Environ. 42, 647–658. https://doi.org/10.1111/pce.13450.

Cui, J., Davantture, M., Zivy, M., Lamade, E., Tcherkez, G., 2019b. Metabolic response to potassium availability and waterlogging reshape respiration and carbon use efficiency in oil palm. New Phytol. 223, 310–322. https://doi.org/10.1111/nph.15751.

Cui, J., Tcherkez, G., 2021. Potassium dependency of enzymes in plant primary metabolism. Plant Physiol. Biochem. 166, 522–530. https://doi.org/10.1016/j.plaphy.2021.06.017.

Da Graça, J.P., Ueda, T.E., Janegitz, T., Vieira, S.S., Salvador, M.C., de Oliveira, M.C.N., Zingaretti, S.M., Powers, S.J., Pickett, J.A., Birkett, M.A., Hoffmann-Campo, C.B., 2016. The natural plant stress elicitor cis-jasmone causes cultivar-dependent reduction in growth of the stink bug, *Euschistus heros* and associated changes in flavonoid concentrations in soybean, *Glycine max*. Phytochemistry 131, 84–91. https://doi.org/10.1016/j.phytochem.2016.08.013.

Davis, J.L., Armengaud, P., Larson, T.R., Graham, I.A., White, P.J., Newton, A.C., Amtmann, A., 2018. Contrasting nutrient-disease relationships: potassium gradients in barley leaves have opposite effects on two fungal pathogens with different sensitivities to jasmonic acid Plant. Cell Environ 41, 2357–2372. https://doi.org/10.1111/pce.13350.

Devi, B.S.R., Kim, Y.J., Selvi, S.K., Gayathri, S., Altanzul, K., Parvin, S., Yang, D.U., Lee, O.R., Lee, S., Yang, D.C., 2012. Influence of potassium nitrate on antioxidant level and secondary metabolite genes under cold stress in *Panax ginseng*. Russ. J. Plant Physiol. 59, 318–325. https://doi.org/10.1134/S1021443712030041.

Diem, B., Godbold, D.L., 1993. Potassium, calcium and magnesium antagonism in clones of *Populus trichocarpa*. Plant Soil 155–156, 411–414. https://doi.org/10.1007/BF00025070.

Dillon, F.M., Chludil, H.D., Zavala, J.A., 2017. Solar UV-B radiation modulates chemical defenses against *Anticarsia gemmatalis* larvae in leaves of field-grown soybean. Phytochemistry 141, 27–36. https://doi.org/10.1016/j.phytochem.2017.05.006.

Fehr, W.R., Caviness, C.E., 1977. Stages of soybean development. Special Report (Iowa State University) 80, 11. https://dr.lib.iastate.edu/handle/20.500.12876/90239.

Feng, Z., Ding, C., Li, W., Wang, D., Cui, D., 2020. Applications of metabolomics in the research of soybean plant under abiotic stress. Food Chem. 310, 125914 https://doi.org/10.1016/j.foodchem.2019.125914.

Firmano, R.F., 2017. Residual effect of potassium fertilization on the nutrient forms in soil. Dissertation (Master's in Soils and Plant Nutrition) – Luiz de Queiroz College of Agriculture. University of Sao Paulo – Brazil. https://doi.org/10.11606/D.11.2017.tde-07062017-090108.

Firmano, R.F., Oliveira, A. de, Castro, C. de, Alleoni, L.R.F., 2020. Potassium rates on the cationic balance of an Oxisol and soybean nutritional status after 8 years of K deprivation. Exp. Agric. 56, 293–311. https://doi.org/10.1017/S0014479719000371.

Foyer, C.H., Lelandais, M., Kunert, K.J., 1994. Photooxidative stress in plants. Physiol. Plantarum 92, 696–717. https://doi.org/10.1111/j.1399-3054.1994.tb03042.x.

Gaaliche, B., Ladhari, A., Zarrelli, A., Ben Mimoun, M., 2019. Impact of foliar potassium fertilization on biochemical composition and antioxidant activity of fig (*Ficus carica* L.). Sci. Hortic. 253, 111–119. https://doi.org/10.1016/j.scienta.2019.04.024.

Gao, X., Zhang, S., Zhao, X., Wu, Q., 2018. Potassium-induced plant resistance against soybean cyst nematode via root exudation of phenolic acids and plant pathogen-related genes. PLoS One 13. https://doi.org/10.1371/journal.pone.0200903.

Graham, T.L., Kim, J.E., Graham, M.Y., 1990. Role of constitutive isoflavone conjugates in the accumulation of glyceollin in soybean infected with *Phytophthora megasperma*. Mol. Plant Microbe Interact. 3, 157. https://doi.org/10.1094/MPMI-3-157.

Hafsi, C., Debez, A., Abdelly, C., 2014. Potassium deficiency in plants: effects and signaling cascades. Acta Physiol. Plant. 36, 1055–1070. https://doi.org/10.1007/s11738-014-1491-2.

Harborne, J.B., Williams, C.A., 2000. Advances in flavonoid research since 1992. Phytochemistry 55, 481–504. https://doi.org/10.1016/S0031-9422(00)00235-1.

Harger, N., 2008. Sufficiency ranges for foliar contents of nutrients in soybean, using the DRIS method, obtained from basalt-derived soils. Thesis (Doctor Degree in Agronomy). State University of Londrina - UEL, Brazil.

Hasanuzzaman, M., Bhuyan, M., Nahar, K., Hossain, Md, Mahmud, J., Hossen, Md, Masud, A., Moumita Fujita, M., 2018. Potassium: a vital regulator of plant responses and tolerance to abiotic stresses. Agronomy 8, 31. https://doi.org/10.3390/agronomy8030031.

Hernandez, M., Fernandez-Garcia, N., Garcia-Garma, J., Rubio-Asensio, J.S., Rubio, F., Olmos, E., 2012. Potassium starvation induces oxidative stress in *Solanum lycopersicum* L. roots. J. Plant Physiol. 169, 1366–1374. https://doi.org/10.1016/j.jplph.2012.05.015.

Herrera, M.D., Acosta-Gallegos, J.A., Reynoso-Camacho, R., Pérez-Ramírez, I.F., 2019. Common bean seeds from plants subjected to severe drought, restricted- and full-irrigation regimes show differential phytochemical fingerprint. Food Chem. 294, 368–377. https://doi.org/10.1016/j.foodchem.2019.05.076.

Hoffmann-Campo, C.B., Harborne, J.B., McCaffery, A.R., 2001. Pre-ingestive and post-ingestive effects of soya bean extracts and rutin on *Trichoplusia ni* growth. Entomol. Exp. Appl. 98, 181–194. https://doi.org/10.1046/j.1570-7458.2001.00773.x.

Hu, W., Yang, J., Meng, Y., Wang, Y., Chen, B., Zhao, W., Oosterhuis, D.M., Zhou, Z., 2015. Potassium application affects carbohydrate metabolism in the leaf subtending the cotton (*Gossypium hirsutum* L.) boll and its relationship with boll biomass. Field Crop. Res. 179, 120–131. https://doi.org/10.1016/j.fcr.2015.04.017.

Huber, D.M., Arny, D.C., 1985. Interactions of potassium with plant disease. In: Munson, R.D. (Ed.), Potassium in Agriculture. American Society of Agronomy, pp. 467–488. https://doi.org/10.2134/1985.potassium.c20.

Issawi, M., Sol, V., Riou, C., 2018. Plant photodynamic stress: what's new? Front. Plant Sci. 9, 1–9. https://doi.org/10.3389/fpls.2018.00681.

Jarvis, P., Dormann, P., Peto, C.A., Lutes, J., Benning, C., Chory, J., 2000. Galactolipid deficiency and abnormal chloroplast development in the *Arabidopsis* MGD synthase 1 mutant. Proc. Natl. Acad. Sci. USA 97, 8175–8179. https://doi.org/10.1073/pnas.100132197.

Keen, N.T., Taylor, O.C., 1975. Ozone injury in soybeans. Plant Physiol. 55, 731–733. https://doi.org/10.1104/pp.55.4.731.

Kuc, J., 1995. Phytoalexins, stress metabolism, and disease resistance in plants. Annu. Rev. Phytopathol. 33, 275–297. https://doi.org/10.1146/annurev.py.33.090195.001423.

Lea, P.J., Sodek, L., Parry, M.A.J., Shewry, P.R., Halford, N.G., 2007. Asparagine in plants. Ann. Appl. Biol. 150, 1–26. https://doi.org/10.1111/j.1744-7348.2006.00104.x.

Lee, C.H., Yang, L., Xu, J.Z., Yeung, S.Y.V.Y., Huang, Y., Chen, Z.-Y., 2005. Relative antioxidant activity of soybean isoflavones and their glycosides. Food Chem. 90, 735–741. https://doi.org/10.1016/j.foodchem.2004.04.034.

Li, H., Yoon, J.-H., Won, H.-J., Ji, H.-S., Yuk, H.J., Park, K.H., Park, H.-Y., Jeong, T.-S., 2017. Isotrifoliol inhibits pro-inflammatory mediators by suppression of TLR/NF-κB and TLR/MAPK signaling in LPS-induced RAW264.7 cells. Int. Immunopharm. 45, 110–119. https://doi.org/10.1016/j.intimp.2017.01.033.

Liu, J., Hu, B., Liu, W., Qin, W., Wu, H., Zhang, J., Yang, C., Deng, J., Shu, K., Du, J., Yang, F., Yong, T., Wang, X., Yang, W., 2017. Metabolomic tool to identify soybean [*Glycine max* (L.) Merrill] germplasms with a high level of shade tolerance at the seedling stage. Sci. Rep. 7, 42478 https://doi.org/10.1038/srep42478.

Liu, Y., Li, M., Xu, J., Liu, X., Wang, S., Shi, L., 2019. Physiological and metabolomics analyses of young and old leaves from wild and cultivated soybean seedlings under low-nitrogen conditions. BMC Plant Biol. 19, 1–15. https://doi.org/10.1186/s12870-019-2005-6.

Lu, Z., Hu, W., Ren, T., Zhu, C., Li, X., Cong, R., Guo, S., Lu, J., 2019. Impact of K deficiency on leaves and siliques photosynthesis via metabolomics in *Brassica napus*. Environ. Exp. Bot. 158, 89–98. https://doi.org/10.1016/j.envexpbot.2018.11.008.

Marschner, P., 2012. Marschner's mineral nutrition of higher plants. third ed.. In: Marschner's Mineral Nutrition of Higher Plants, third ed. Elsevier. https://doi.org/10.1016/C2009-0-63043-9.

Marschner, H., Cakmak, I., 1989. High light intensity enhances chlorosis and necrosis in leaves of zinc, potassium, and magnesium deficient bean (*Phaseolus vulgaris*) Plants. J. Plant Physiol. 134, 308–315. https://doi.org/10.1016/S0176-1617(89)80248-2.

Marschner, H., Kirkby, E.A., Cakmak, I., 1996. Effect of mineral nutritional status on shoot-root partitioning of photoassimilates and cycling of mineral nutrients. J. Exp. Bot. 47, 1255–1263. https://doi.org/10.1093/jxb/47.Special_Issue.1255.

Malavolta, E., 1980. Elementos de nutrição mineral de plantas. Agronômica Ceres, São Paulo.

Malvi, U.R., 2011. Interaction of micronutrients with major nutrients with special reference to potassium. Karnataka J. Agri. Sci. 24 (1), 106–109.

Mehlich, A., 1953. Determination of P, Ca, Mg, K, Na, and NH_4. In: Short test methods used in soil testing division. North Carolina Soil Test Division, Raleigh, p. 8.

Mehlich, A., 1984. Mehlich 3 soil test extractant: a modification of Mehlich 2 extractant. Commun. Soil Sci. Plant Anal. 15, 1409–1416. https://doi.org/10.1080/00103628409367568.

Mengel, K., Kirkby, E.A., Kosegarten, H., Appel, T. (Eds.), 2001. Principles of Plant Nutrition, fifth ed. Springer Netherlands, Dordrecht. https://doi.org/10.1007/978-94-010-1009-2.

Meyer, M.C., Klepker, D., 2007. Management of anthracnose on soybean crop. In: XL Brazilian Congress of Phytopathology - Maringá, 32. Braz. Phytopathol., Brazil, pp. 31–33.

Miao, B.-H., Han, X.-G., Zhang, W.-H., 2010. The ameliorative effect of silicon on soybean seedlings grown in potassium-deficient medium. Ann. Bot. 105, 967–973. https://doi.org/10.1093/aob/mcq063.

Moran, J.F., Klucas, R.V., Grayer, R.J., Abian, J., Becana, M., 1997. Complexes of iron with phenolic compounds from soybean nodules and other legume tissues: prooxidant and antioxidant properties. Free Radic. Biol. Med. 22, 861–870. https://doi.org/10.1016/S0891-5849(96)00426-1.

Mugnai, S., Marras, A.M., Mancuso, S., 2011. Effect of hypoxic acclimation on anoxia tolerance in *Vitis* roots: response of metabolic activity and K^+ fluxes. Plant Cell Physiol. 52, 1107–1116. https://doi.org/10.1093/pcp/pcr061.

Murakami, S., Nakata, R., Aboshi, T., Yoshinaga, N., Teraishi, M., Okumoto, Y., Ishihara, A., Morisaka, H., Huffaker, A., Schmelz, E., Mori, N., 2014. Insect-induced daidzein, formononetin and their conjugates in soybean leaves. Metabolites 4, 532–546. https://doi.org/10.3390/metabo4030532.

Murakawa, M., Shimojima, M., Shimomura, Y., Kobayashi, K., Awai, K., Ohta, H., 2014. Monogalactosyldiacylglycerol synthesis in the outer envelope membrane of chloroplasts is required for enhanced growth under sucrose supplementation. Front. Plant Sci. 5, 1–13. https://doi.org/10.3389/fpls.2014.00280.

Nguyen, P.M., Kwee, E.M., Niemeyer, E.D., 2010. Potassium rate alters the antioxidant capacity and phenolic concentration of basil (*Ocimum basilicum* L.) leaves. Food Chem. 123, 1235–1241. https://doi.org/10.1016/j.foodchem.2010.05.092.

Nothias, L.-F., Petras, D., Schmid, R., Dührkop, K., Rainer, J., Sarvepalli, A., Protsyuk, I., Ernst, M., Tsugawa, H., Fleischauer, M., Aicheler, F., Aksenov, A.A., Alka, O., Allard, P.-M., Barsch, A., Cachet, X., Caraballo-Rodriguez, A.M., Da Silva, R.R., Dang, T., Garg, N., Gauglitz, J.M., Gurevich, A., Isaac, G., Jarmusch, A.K., Kameník, Z., Kang, K. Bin, Kessler, N., Koester, I., Korf, A., Le Gouellec, A., Ludwig, M., Martin, H.C., McCall, L.-I., McSayles, J., Meyer, S.W., Mohimani, H., Morsy, M., Moyne, O., Neumann, S., Neuweger, H., Nguyen, N.H., Nothias-Esposito, M., Paolini, J., Phelan, V.V., Pluskal, T., Quinn, R.A., Rogers, S., Shrestha, B., Tripathi, A., van der Hooft, J.J.J., Vargas, F., Weldon, K.C., Witting, M., Yang, H., Zhang, Z., Zubeil, F., Kohlbacher, O., Böcker, S., Alexandrov, T., Bandeira, N., Wang, M., Dorrestein, P.C., 2020. Feature-based molecular networking in the GNPS analysis environment. Nat. Methods 17, 905–908. https://doi.org/10.1038/s41592-020-0933-6.

Okubo, K., Yoshiki, Y., 2000. The role of triterpenoid on reactive oxygen scavenging system: approach from the new chemiluminescence system (XYZ system). Biofactors 13, 219–223. https://doi.org/10.1002/biof.5520130134.

Oliveira Junior, A., Castro, C., Oliveira, F.A., Klepker, D., 2020. Fertilidade do solo e avalição do estado nutricional da Soja. In: Seixas, C.D.S., Neumaier, N., Balbinot Junior, A.A., Krzyzanowski, F.C., Leite, R.M.V.B.C. (Eds.), Tecnologias de produção de soja. Embrapa Soja, Londrina, pp. 133–184. ISSN 2176-2902.

Pandey, G.K., Mahiwal, S., 2020. Role of potassium in plants. In: Springer Briefs in Plant Science. Springer International Publishing, Cham. https://doi.org/10.1007/978-3-030-45953-6.

Parvej, M.R., Slaton, N.A., Purcell, L.C., Roberts, T.L., 2015. Potassium fertility effects yield components and seed potassium concentration of determinate and indeterminate soybean. Agron. J. 107, 943–950. https://doi.org/10.2134/agronj14.0464.

Pauletti, V., Motta, A.C.V., 2019. Manual de adubação e calagem para o estado do paraná, 2nd. Sociedade Brasileira de Ciência do Solo - Núcleo Estadual Paraná, Curitiba.

Perrenoud, S., 1990. Potassium and plant health. International Potash Institute Bern, Switzerland 2, 7–12. EPI Research Topics, 3.

Piubelli, G.C., Hoffmann-Campo, C.B., de Arruda, I.C., Franchini, J.C., Lara, F.M., 2003. Flavonoid increase in soybean as a response to *Nezara viridula* injury and its effect on insect-feeding preference. J. Chem. Ecol. 29, 1223–1233. https://doi.org/10.1023/A:1023889825129.

Piubelli, G.C., Hoffmann-Campo, C.B., Moscardi, F., Miyakubo, S.H., Neves De Oliveira, M.C., 2005. Are chemical compounds important for soybean resistance to *Anticarsia gemmatalis*? J. Chem. Ecol. 31, 1509–1525. https://doi.org/10.1007/s10886-005-5794-z.

Pospíšil, P., 2016. Production of reactive oxygen species by photosystem II as a response to light and temperature stress. Front. Plant Sci. 7, 1–12. https://doi.org/10.3389/fpls.2016.01950.

Potash Phosphate Institute, 1998. Effects of potassium on plant diseases. Better Crops with Plant Food. Norcross, Georgia, USA. 82 (3), 37–39. ISSN 0006-0089.

Prasad, D., Singh, A., Singh, R., 2010. Management of sheath blight of rice with integrated nutrients. Indian Phytopathol. 63 (1), 11–15.

Rice-Evans, C., Miller, N., Paganga, G., 1997. Antioxidant properties of phenolic compounds. Trends Plant Sci. 2, 152–159. https://doi.org/10.1016/S1360-1385(97)01018-2.

Rubin, B., Penner, D., Saettler, A.W., 1983. Induction of isoflavonoid production in *Phaseolus Vulgaris* L. leaves by ozone, sulfur dioxide and herbicide stress. Environ. Toxicol. Chem. 2, 295–306. https://doi.org/10.1002/etc.5620020305.

Schrimpe-Rutledge, A.C., Codreanu, S.G., Sherrod, S.D., McLean, J.A., 2016. Untargeted metabolomics strategies - challenges and emerging directions. J. Am. Soc. Mass Spectrom. 27, 1897–1905. https://doi.org/10.1007/s13361-016-1469-y.

Seguin, P., Zheng, W., 2006. Potassium, phosphorus, sulfur, and boron fertilization effects on soybean isoflavone content and other seed characteristics. J. Plant Nutr. 29, 681–698. https://doi.org/10.1080/01904160600564477.

Seixas, C.D.S., Soares, R.M., Godoy, C.V., Meyer, M.C., Costamilan, L.M., Dias, W.P., Almeida, Á.M.R., 2020. Manejo de doenças. In: Seixas, C.D.S., Neumaier, N., Junior, A.A.B., Krzyzanowski, F.C., Leite, R.M. (Eds.), Tecnologias de produção de soja. Embrapa Soja, Londrina, pp. 227–264. ISSN 2176-2902.

Severtson, D., Callow, N., Flower, K., Neuhaus, A., Olejnik, M., Nansen, C., 2016. Unmanned aerial vehicle canopy reflectance data detects potassium deficiency and green peach aphid susceptibility in canola. Precis. Agric. 17, 659–677. https://doi.org/10.1007/s11119-016-9442-0.

Shankar, A., Singh, A., Kanwar, P., Srivastava, A.K., Pandey, A., Suprasanna, P., Kapoor, S., Pandey, G.K., 2013. Gene expression analysis of rice seedling under potassium deprivation reveals major changes in metabolism and signaling components. PLoS One 8, e70321. https://doi.org/10.1371/journal.pone.0070321.

Shannon, P., Markiel, A., Ozier, O., Baliga, N.S., Wang, J.T., Ramage, D., Amin, N., Schwikowski, B., Ideker, T., 2003. Cytoscape: a software environment for integrated models of biomolecular interaction networks. Genome Res. 13, 2498–2504. https://doi.org/10.1101/gr.1239303.

Shen, W., Guo, R., Zhao, Y., Liu, D., Chen, J., Miao, N., Gao, S., Zhang, T., Shi, L., 2021. Nutrient reabsorption mechanism adapted to low phosphorus in wild and cultivated soybean varieties. J. Plant Growth Regul. https://doi.org/10.1007/s00344-021-10495-z.

Simons, R., Vincken, J.-P., Roidos, N., Bovee, T.F.H., van Iersel, M., Verbruggen, M.A., Gruppen, H., 2011. Increasing soy isoflavonoid content and diversity by simultaneous malting and challenging by a fungus to modulate estrogenicity. J. Agric. Food Chem. 59, 6748–6758. https://doi.org/10.1021/jf2010707.

Soil Survey Staff, 2014. Keys to soil taxonomy, 14th. Department of Agriculture (USDA) Natural Resources Conservation Service, Washington, DC.

Song, H.-H., Ryu, H.W., Lee, K.J., Jeong, I.Y., Kim, D.S., Oh, S.-R., 2014. Metabolomics investigation of flavonoid synthesis in soybean leaves depending on the growth stage. Metabolomics 10, 833–841. https://doi.org/10.1007/s11306-014-0640-3.

Stewart, G.R., Larher, F., 1980. Accumulation of amino acids and related compounds in relation to environmental stress. In: Amino Acids and Derivatives. Elsevier, pp. 609–635. https://doi.org/10.1016/B978-0-12-675405-6.50023-1.

Sumner, L.W., Amberg, A., Barrett, D., Beale, M.H., Beger, R., Daykin, C.A., Fan, T.W.M., Fiehn, O., Goodacre, R., Griffin, J.L., Hankemeier, T., Hardy, N., Harnly, J., Higashi, R., Kopka, J., Lane, A.N., Lindon, J.C., Marriott, P., Nicholls, A.W., Reily, M.D., Thaden, J.J., Viant, M.R., 2007. Proposed minimum reporting standards for chemical analysis. Metabolomics 3, 211–221. https://doi.org/10.1007/s11306-007-0082-2.

Szakiel, A., Pączkowski, C., Henry, M., 2011. Influence of environmental abiotic factors on the content of saponins in plants. Phytochemistry Rev. 10, 471–491. https://doi.org/10.1007/s11101-010-9177-x.

Tantriani, T.S., Cheng, W., Saito, K., Oikawa, A., Purwanto, B.H., Tawaraya, K., 2020. Metabolomic analysis of night-released soybean root exudates under high- and low-K conditions. Plant Soil 456, 259–276. https://doi.org/10.1007/s11104-020-04715-w.

Tiku, A.R., 2020. Antimicrobial compounds (phytoanticipins and phytoalexins) and their role in plant defense. In: Mérillon, J.-M., Ramawat, K.G. (Eds.), Co-Evolution of Secondary Metabolites. Springer Nature Switzerland, Gewerbestrasse, pp. 845–868. https://doi.org/10.1007/978-3-319-96397-6_63.

Toda, S., Shirataki, Y., 1999. Inhibitory effects of isoflavones on lipid peroxidation by reactive oxygen species. Phytother Res. 13, 163–165. https://doi.org/10.1002/(SICI)1099-1573(199903)13:2%3C163::AID-PTR405%3E3.0.CO;2-#.

Tripathi, D.K., Singh, Shweta, Gaur, S., Singh, Swati, Yadav, V., 2018. Acquisition and homeostasis of iron in higher plants and their probable role in abiotic stress tolerance. Front. Environ. Sci. 5, 1–15. https://doi.org/10.3389/fenvs.2017.00086.

Troufflard, S., Mullen, W., Larson, T.R., Graham, I.A., Crozier, A., Amtmann, A., Armengaud, P., 2010. Potassium deficiency induces the biosynthesis of oxylipins and glucosinolates in Arabidopsis thaliana. BMC Plant Biol. 10, 172. https://doi.org/10.1186/1471-2229-10-172.

Tsugawa, H., Cajka, T., Kind, T., Ma, Y., Higgins, B., Ikeda, K., Kanazawa, M., VanderGheynst, J., Fiehn, O., Arita, M., 2015. MS-DIAL: data-independent MS/MS deconvolution for comprehensive metabolome analysis. Nat. Methods 12, 523–526. https://doi.org/10.1038/nmeth.3393.

Tsugawa, H., Kind, T., Nakabayashi, R., Yukihira, D., Tanaka, W., Cajka, T., Saito, K., Fiehn, O., Arita, M., 2016. Hydrogen rearrangement rules: computational MS/MS

fragmentation and structure elucidation using MS-FINDER software. Anal. Chem. 88, 7946–7958. https://doi.org/10.1021/acs.analchem.6b00770.
Tsugawa, H., Nakabayashi, R., Mori, T., Yamada, Y., Takahashi, M., Rai, A., Sugiyama, R., Yamamoto, H., Nakaya, T., Yamazaki, M., Kooke, R., Bac-Molenaar, J. A., Oztolan-Erol, N., Keurentjes, J.J.B., Arita, M., Saito, K., 2019. A cheminformatics approach to characterize metabolomes in stable-isotope-labeled organisms. Nat. Methods 16, 295–298. https://doi.org/10.1038/s41592-019-0358-2.
Tsuno, Y., Fujimatsu, T., Endo, K., Sugiyama, A., Yazaki, K., 2018. Soyasaponins: a new class of root exudates in soybean (*Glycine max*). Plant Cell Physiol. 59, 366–375. https://doi.org/10.1093/pcp/pcx192.
Tugizimana, F., Steenkamp, P., Piater, L., Dubery, I., 2016. A conversation on data mining strategies in LC-MS untargeted metabolomics: pre-processing and pre-treatment Steps. Metabolites 6, 40. https://doi.org/10.3390/metabo6040040.
USPEA, 1996. Soil screening guidance: technical background document, 2nd. Office of Solid Waste and Emergency Response, Washington, DC.
Vanderplanck, M., Glauser, G., 2018. Integration of non-targeted metabolomics and automated determination of elemental compositions for comprehensive alkaloid profiling in plants. Phytochemistry 154, 1–9. https://doi.org/10.1016/j.phytochem.2018.06.011.
VanToai, T.T., Lee, J.-D., Goulart, P.F.P., Shannon, G.J., Alves, D.J., Nguyen, H.T., Yu, O., Rahman, M., Islam, R., 2012. Soybean (*Glycine max* L. Merr.) seed composition response to soil flooding stress. J. Food Agric. Environ. 10 (1), 795–801.
Vyn, T.J., Yin, X., Bruulsema, T.W., Jackson, C.-J.C., Rajcan, I., Brouder, S.M., 2002. Potassium fertilization effects on isoflavone concentrations in soybean [*Glycine max* (L.) Merr.]. J. Agric. Food Chem. 50, 3501–3506. https://doi.org/10.1021/jf0200671.
Wade, A.M., Tucker, H.N., 1998. Antioxidant characteristics of *L*-histidine. J. Nutr. Biochem. 9, 308–315. https://doi.org/10.1016/S0955-2863(98)00022-9.
Walkley, A., Black, I.A., 1934. An examination of the Degtjareff method for determining soil organic matter, and a proposed modification of the chromic acid titration method. Soil Sci. 37, 29–38. https://doi.org/10.1097/00010694-193401000-00003.
Walter, A.J., DiFonzo, C.D., 2007. Soil potassium deficiency affects soybean phloem nitrogen and soybean aphid populations. Environ. Entomol. 36, 26–33. https://doi.org/10.1603/0046-225X.
Wang, M., Zheng, Q., Shen, Q., Guo, S., 2013. The critical role of potassium in plant stress response. Int. J. Mol. Sci. 14, 7370–7390. https://doi.org/10.3390/ijms14047370.
Wang, M., Carver, J.J., Phelan, V.V., Sanchez, L.M., Garg, N., Peng, Y., Nguyen, D.D., Watrous, J., Kapono, C.A., Luzzatto-Knaan, T., Porto, C., Bouslimani, A., Melnik, A. V., Meehan, M.J., Liu, W.-T., Crüsemann, M., Boudreau, P.D., Esquenazi, E., Sandoval-Calderón, M., Kersten, R.D., Pace, L.A., Quinn, R.A., Duncan, K.R., Hsu, C.-C., Floros, D.J., Gavilan, R.G., Kleigrewe, K., Northen, T., Dutton, R.J., Parrot, D., Carlson, E.E., Aigle, B., Michelsen, C.F., Jelsbak, L., Sohlenkamp, C., Pevzner, P., Edlund, A., McLean, J., Piel, J., Murphy, B.T., Gerwick, L., Liaw, C.-C., Yang, Y.-L., Humpf, H.-U., Maansson, M., Keyzers, R.A., Sims, A.C., Johnson, A.R., Sidebottom, A.M., Sedio, B.E., Klitgaard, A., Larson, C.B., Boya P, C.A., Torres-Mendoza, D., Gonzalez, D.J., Silva, D.B., Marques, L.M., Demarque, D.P., Pociute, E., O'Neill, E.C., Briand, E., Helfrich, E.J.N., Granatosky, E.A., Glukhov, E., Ryffel, F., Houson, H., Mohimani, H., Kharbush, J.J., Zeng, Y., Vorholt, J.A., Kurita, K.L., Charusanti, P., McPhail, K.L., Nielsen, K.F., Vuong, L., Elfeki, M., Traxler, M.F., Engene, N., Koyama, N., Vining, O.B., Baric, R., Silva, R.R., Mascuch, S.J., Tomasi, S., Jenkins, S., Macherla, V., Hoffman, T., Agarwal, V., Williams, P.G., Dai, J., Neupane, R., Gurr, J., Rodríguez, A.M.C., Lamsa, A., Zhang, C., Dorrestein, K., Duggan, B.M., Almaliti, J., Allard, P.-M., Phapale, P., Nothias, L.-F., Alexandrov, T., Litaudon, M., Wolfender, J.-L., Kyle, J.E., Metz, T.O., Peryea, T., Nguyen, D.-T., VanLeer, D., Shinn, P., Jadhav, A., Müller, R., Waters, K.M., Shi, W., Liu, X., Zhang, L., Knight, R., Jensen, P.R., Palsson, B.Ø., Pogliano, K., Linington, R. G., Gutiérrez, M., Lopes, N.P., Gerwick, W.H., Moore, B.S., Dorrestein, P.C., Bandeira, N., 2016. Sharing and community curation of mass spectrometry data with global natural products social molecular networking. Nat. Biotechnol. 34, 828–837. https://doi.org/10.1038/nbt.3597.
Weinert, C.H., Sonntag, F., Egert, B., Pawelzik, E., Kulling, S.E., Smit, I., 2021. The effect of potassium fertilization on the metabolite profile of tomato fruit (*Solanum lycopersicum* L.). Plant Physiol. Biochem. 19, 89–99. https://doi.org/10.1016/j.plaphy.2020.12.010.
Wu, W., Zhang, Q., Zhu, Y., Lam, H.-M., Cai, Z., Guo, D., 2008. Comparative metabolic profiling reveals secondary metabolites correlated with soybean salt tolerance. J. Agric. Food Chem. 56, 11132–11138. https://doi.org/10.1021/jf8024024.
Yang, L., Wen, K.S., Ruan, X., Zhao, Y.X., Wei, F., Wang, Q., 2018. Response of plant secondary metabolites to environmental factors. Molecules 23, 762. https://doi.org/10.3390/molecules23040762.
Yates, P.S., Roberson, J., Ramsue, L.K., Song, B.-H., 2021. Bridging the gaps between plant and human health: a systematic review of soyasaponins. J. Agric. Food Chem. 69, 14387–14401. https://doi.org/10.1021/acs.jafc.1c04819.
Yoshiki, Y., Okubo, K., 1995. Active oxygen scavenging activity of DDMP (2,3-Dihydro-2,5-dihydroxy-6-methyl-4*H*-pyran-4-one) saponin in soybean seed. Biosci. Biotechnol. Biochem. 59, 1556–1557. https://doi.org/10.1271/bbb.59.1556.
Yoshiki, Y., Kudou, S., Okubo, K., 1998. Relationship between chemical structures and biological activities of triterpenoid saponins from soybean. Biosci. Biotechnol. Biochem. 62, 2291–2299. https://doi.org/10.1271/bbb.62.2291.
Yuk, H.J., Curtis-Long, M.J., Ryu, H.W., Jang, K.C., Seo, W.D., Kim, J.Y., Kang, K.Y., Park, K.H., 2011. Pterocarpan profiles for soybean leaves at different growth stages and investigation of their glycosidase inhibitions. J. Agric. Food Chem. 59, 12683–12690. https://doi.org/10.1021/jf203326c.
Zhao, M., Guo, R., Li, M., Liu, Y., Wang, X., Fu, H., Wang, S., Liu, X., Shi, L., 2020. Physiological characteristics and metabolomics reveal the tolerance mechanism to low nitrogen in *Glycine soja* leaves. Physiol. Plantarum 168, 819–834. https://doi.org/10.1111/ppl.13022.
Zhao, S.-Y., Liu, Z.-L., Shu, Y.-S., Wang, M.-L., He, D., Song, Z.-Q., Zeng, H.-L., Ning, Z.-C., Lu, C., Lu, A.-P., Liu, Y.-Y., 2017. Chemotaxonomic classification applied to the identification of two closely-related Citrus TCMs using UPLC-Q-TOF-MS-based metabolomics. Molecules 22, 1721. https://doi.org/10.3390/molecules22101721.
Zhu, H., Lin, H., Tan, J., Wang, C., Wang, H., Wu, F., Dong, Q., Liu, Y., Li, P., Liu, J., 2018. UPLC-QTOF/MS-based nontargeted metabolomic analysis of mountain- and garden-cultivated ginseng of different ages in Northeast China. Molecules 24, 33. https://doi.org/10.3390/molecules24010033.
Zs-Nagy, I., Floyd, R.A., 1984. Hydroxyl free radical reactions with amino acids and proteins studied by electron spin resonance spectroscopy and spin-trapping. Biochim. Biophys. Acta Protein Struct. Mol. Enzymol. 790, 238–250. https://doi.org/10.1016/0167-4838(84)90028-1.